Journal of Proteomics 287 (2023) 104997

Contents lists available at ScienceDirect

Journal of Proteomics

journal homepage: www.elsevier.com/locate/jprot

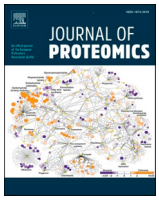

In-depth characterization of the sarcoplasmic muscle proteome changes in lambs fed with hazelnut skin by-products: Relationships with meat color

Antonella della Malva [a,**], Mohammed Gagaoua [b,*], Antonella Santillo [a], Martina di Corcia [a], Antonio Natalello [c], Agostino Sevi [a], Marzia Albenzio [a]

[a] Department of Agriculture, Food, Natural Resources and Engineering (DAFNE), University of Foggia, Via Napoli 25, 71121 Foggia, Italy
[b] PEGASE, INRAE, Institut Agro, 35590 Saint-Gilles, France
[c] Department of Agriculture, Food and Environment (Di3A), University of Catania, Via Valdisavoia 5, 95123 Catania, Italy

ARTICLE INFO

Keywords:
Lamb meat color
Muscle proteome
Sarcoplasmic proteins
Molecular pathways
Feeding strategies
Bioinformatics

ABSTRACT

This study investigated the effect of agro-industrial hazelnut skin by-products supplementation on lamb meat color variation and the changes in the sarcoplasmic muscle proteome during post-mortem storage (0, 4 and 7 days). Gel-based proteomics and bioinformatics approaches were applied to better understand the potential role of feeding strategies in modulating the mechanisms underpinning meat discoloration and post-mortem changes during storage. Therefore, twenty-two Valle del Belice male lambs were randomly assigned to two dietary treatments: control (C), lambs fed with maize-barley diet, and hazelnut skin (H), lambs fed hazelnut skin by-product as maize partial replacer in the concentrate diet. Hazelnut dietary treatment led to better lamb meat color stability as evidenced by the lowest decrease in redness and saturation index values. Proteomics and bioinformatics results revealed changes in the abundance of 41 proteoforms, which were mainly involved in glycolytic processes, responses to oxidative stress, and immune and endocrine system. The proteins allowed revealing interconnected pathways to be behind meat color variation as a consequence of using hazelnut skin by-products to sustainable feed lamb. The proteins can be used as potential predictors of lamb meat color variation. Accordingly, the regression equations developed in this paper revealed triosephosphate isomerase (TPI1) as a reliable candidate biomarker of color stability in lamb meat.

Significance: The use of agro-industrial by-products in animal feeding can be a potential sustainable strategy to reduce the environmental impacts of the food production chain and consequently improve animal welfare and product quality. The inclusion of hazelnut skin by-products in the animal's diet, due to the high concentration of polyphenols, represents an effective strategy to improve the oxidative stability of meat, with significant implications on color. The use of proteomics combined with bioinformatics on the sarcoplasmic proteome is a powerful approach to decipher the underlying mechanism. Accordingly, this approach allowed in this trial a deeper understanding of the molecular mechanisms involved in the post-mortem processes through the discovery of several biological pathways linked with lamb meat color variation. Glycolysis, followed by responses to oxidative stress, and other proteins involved in the immune and endocrine system were found as the major interconnected pathways that could act as potential predictors of lamb meat color stability. Candidate proteins biomarkers were further revealed in this study to be related with multiple meat color traits.

1. Introduction

Among meat sensory traits, color is the primary attribute used by consumers for the purchase at the point of sale, hence influencing meat marketability [1,2]. Therefore, explaining the mechanisms involved in meat color variation is of importance for the meat industry from an economic perspective point of view [3,4]. Throughout storage stage, red fresh meats inevitably undergo different color changes as a consequence of sophisticated biochemical processes [5]. Among them, oxidation and free oxygenated radicals' accumulation can reduce the activities of the intrinsic antioxidant defense systems leading to oxidative damage, both in lipids and proteins [2,5,6] with an impact on meat color stability and

* Corresponding author.
** Corresponding author
E-mail addresses: antonella.dellamalva@unifg.it (A. della Malva), mohammed.gagaoua@inrae.fr (M. Gagaoua).

https://doi.org/10.1016/j.jprot.2023.104997
Received 25 May 2023; Received in revised form 15 August 2023; Accepted 18 August 2023
Available online 30 August 2023
1874-3919/© 2023 Elsevier B.V. All rights reserved.

discoloration. Myoglobin (Mb) is the primary sarcoplasmic protein that determines meat color. It is well known that the exposure of prooxidant molecules can destabilize Mb, hence leading to oxidation of the iron forms to the ferric state with consequent accumulation of metmyoglobin (MMb). Due to their ability to interact directly with myoglobin, the sarcoplasmic proteins, which contain several metabolic enzymes, heat shock proteins, and oxidative stress proteins play a pivotal role in the myriad biochemical processes influencing meat color variation and stability [1,7–10].

Polyphenols can prevent or delay the oxidation processes due to their role in chelating transition metal ions, scavenging free radicals, and removing carbonyl compounds [11,12]. The effectiveness of using polyphenols in the animals' diet as a strategy to prevent and reduce meat oxidation processes, hence improving the final quality of meat has been demonstrated [13,14]. In particular, polyphenols-diet supplementation in ruminants has been investigated for their ability to improve the oxidative stability of meat, with significant implications on color [15] and flavour [16]. Among the agro-industrial by-products, hazelnut (*Corylus avellana L.*) skin is an important source of polyphenols, largely represented by condensed tannins with significant amounts compared to nuts [17]. Recently, authors investigated the effect of dietary hazelnut skin supplementation in growing lambs [18,19]. The authors evidenced an improvement of meat nutritional characteristics mainly through a significant increase in health-promoting fatty acids. In another study under the same experimental design, Menci et al. [20] observed that feeding hazelnut skin can improve the oxidative stability of lamb meat by delaying lipid oxidation due to their higher tocopherols and phenolic compounds content. Although the demonstrated antioxidant potential of the hazelnut skin, the molecular mechanisms underlying meat color variation related to protein and lipid oxidation processes remain unknown.

With the rapid development of analytical techniques, proteomics combined with bioinformatics tools allow a deeper understanding of the molecular mechanisms involved in the post-mortem processes through the discovery of several biological pathways involved in the development of meat quality traits [1,21]. Recently, high-resolution mass spectrometry techniques can provide new insights, including the accurate identification of specific proteins and proteoforms, making it an ideal investigative tool for muscle biomarkers discovery for determining the molecular mechanisms underpinning the conversion of muscle into meat. In the last years, proteomics-based techniques combined with mass spectrometry have been employed to investigate the dynamic changes and modifications occurring in post-mortem muscle in link with meat color traits in beef [22–24], pork [25], horse [26] and lamb [27–29]. Indeed, at present, proteomics allowed to discover and confirm biomarkers linked with different meat color parameters as evidenced in the recent integromics study by Gagaoua et al. [1]. However, to the best of our knowledge, no data are yet available on the use of proteomics to investigate the effect of hazelnut skin-diet supplementation on the post-mortem processes and changes underpinning the variation of meat color through the sarcoplasmic muscle proteome. In this context, we suppose that a better understanding of the sarcoplasmic proteomic changes and the biochemical pathways related to the antioxidant ability of hazelnut skin by-product compounds could be useful for the development of specific strategies aiming at the improvement of the organoleptic quality of lamb meat, in a context of a circular economy. Thus, the main objectives of the present study were first to investigate the changes of the sarcoplasmic proteome of meat from lambs fed with a hazelnut skin by-product during storage using gel-based proteomics and bioinformatics approaches. Second, the trial aimed assessing the relationships between meat color traits and proteome changes to decipher the underlying mechanisms related to lamb meat color variation, while considering multiple color traits.

2. Materials and methods

2.1. Animals, dietary treatments, and meat sampling

The experimental trial was carried out in Sicily Region at the experimental farm of the University of Catania (37°24′35.3"N 15°03′34.9″E). All experimental procedures were accomplished following the European Union Guidelines (2010/63/ EU Directive) and approved by the Ethical and Animal Well-being Commission of the University of Catania (Protocol number 15295). Details of the experimental design were previously described [18]. Briefly, the experiment used 22 Valle del Belice male lambs (60 ± 4 days of age) that were randomly assigned to two dietary treatments. A "control (C)" of the lambs fed with basal diet (maize-barley based concentrate), and the treatment "hazelnut skin (H)" of the lambs fed with the same diet but 150 g/kg dry matter (DM) of maize was replaced with hazelnut skin by-product. Details of the ingredients, chemical composition, and fatty acid profile of diets are reported in a recently published companion paper [18]. During the experimental period, animals were fed in individual pens (1.5 m^2) with straw litter equipped with clean water all the time.

After 56 days of experimental trial, animals were transported to a commercial abattoir (approximately 45 min of transport duration) in accordance with the Council Regulation EC No 1/2005 on the protection of animals during transport. Before slaughter, all lambs were kept in a lairage for 10–12 h overnight without feed but with free access to water. Then, animals were slaughtered following industrial practices used in Italy and in line with European guidelines (EU rule n. 1099/2009). Each carcass was weighed and chilled at 2–4 °C for 24 h. The effect of dietary treatment on growth performance and intakes were reported in the companion paper [18]. After 24 h post-mortem, carcasses were halved and the entire *Longissimus thoracis et lumborum* muscle (LTL) was excised from both sides. From the right LTL, three slices (2 cm thickness) were cut and placed in polystyrene trays, covered with oxygen-permeable PVC film, and stored in the dark at 4 °C for 0 (24 h post-mortem), 4 and 7 days. At each storage time, the color and metmyoglobin percentage of fresh lamb meat were determined. Subsequently, meat samples obtained at each sampling time were collected, immediately frozen in liquid nitrogen, and stored at −80 °C until further proteome analysis.

2.2. Instrumental color and metmyoglobin measurement

Color stability in raw meat over aerobic refrigerated storage was measured as described by Valenti et al. [30]. In brief, at the end of the respective storage time, the PVC film was removed, and each steak was allowed to bloom at chilled temperature (3–4 °C) for 2 h prior to color measurement by using a Minolta CM 2022 spectrophotometer (8 mm diameter aperture with a closed cone, illuminant A, 10° standard observer, d/8° geometry; Minolta Co. Ltd. Osaka, Japan) set to operate in the specular components excluded (SCE) mode. Three measurements were taken on the meat surface and the mean value was calculated. The color descriptors lightness (L^*), redness (a^*), and yellowness (b^*) were determined in the CIE $L^* a^* b^*$ color space. Subsequently, the saturation (C*) and hue angle (h°) were further calculated as in Gagaoua et al. [31]. Reflectance spectrum from 400 nm to 700 nm was recorded for the calculation of metmyoglobin, expressed as a percentage of the total forms of myoglobin as described earlier by Krzywicki [32] and Menci et al. [20]. Furthermore, metmyoglobin accumulation at the meat surface was determined by calculating the ratio between absorption coefficient and scattering coefficient (K/S) at isosbestic wavelengths (525, 572, and 610 nm) for each myoglobin redox form. K/S ratio at the selected wavelengths was calculated as follow:

$$(K/S)_\lambda = (1 - R_\lambda)^2 / 2R_\lambda$$

The ratio of the reflectance (R) values at 630 nm and 580 nm (R630/R580) has been also calculated as a known indicator of the oxidation

process [33].

2.3. Sarcoplasmic muscle proteome analysis

2.3.1. Protein extraction and separation using 1D SDS-PAGE electrophoresis

The extraction of sarcoplasmic proteins was based on the method described by Marino et al. [34]. The LTL samples ($n = 22$, eleven for control and hazelnut, respectively) on each storage day (0, 4, and 7 days) were used. Briefly, 2.5 g of each muscle was homogenized in 10 mL of phosphate buffer (pH 7) containing a protease inhibitor cocktail (P2714, Sigma-Aldrich, St. Louis, MO, USA) by means of an Ultra Turrax at 10 000 RPM during 3 min. The homogenates were then centrifuged (8000 *xg* for 20 min at 4 °C) and the supernatants corresponding to the sarcoplasmic proteins were collected and stored at −80 °C. The protein concentration was determined in duplicate employing the 2-D Quant kit (GE Healthcare, Upsala, Sweden) and bovine serum albumin (BSA) as standard.

Sarcoplasmic proteins were separated using one-dimensional sodium dodecyl sulfate-polyacrylamide gel electrophoresis (1D SDS-PAGE) in 8–18% gradient gel loaded with 90 μg of protein/well. The run was performed in a continuous buffer system using a Protean II xi vertical slab gel unit system (Bio-Rad Laboratories) at 30 mA/gel until the bromophenol blue marker reached the bottom of the gel. Known molecular weight standards (Precision Plus protein standard-broad range, Bio-Rad, Laboratories, Hercules, CA) were added in the first wells. The gels were stained with Coomassie Blue G 250 and, after destaining, analyzed with the Image lab software (version 5.2.1, Bio-Rad Laboratories) to determine the percentage of the signal intensity of the changing and targeted bands. The identification of the protein bands of interest has been conducted through qualitative analysis using MALDI-TOF on the analyzed gels in line with internal gel maps. The internal maps help the confirmation of the results to overcome several gels analyses. The 1D protein bands abundances allowed the analysis of the whole samples (22 animals) with required repeatability ($n = 33$ gels) with less bias compared to 2D gels, thanks to the reference maps.

2.3.2. Two-dimensional gel electrophoresis (2DE) and image analysis

Two-dimensional gel electrophoresis (2DE) was conducted according to Della Malva et al. [26]. Briefly, for the first dimension, the isoelectric focusing (IEF) was carried out using immobilized pH gradient dry strips (IPG) of pH 3–10 linear range, 17 cm long (Bio-Rad Laboratories, Hercules, CA) loaded with 300 μg of sarcoplasmic protein extract dissolved in rehydration sample buffer (ready-Prep Rehydration/Sample Buffer, Bio-Rad). The IEF was carried out at 20 °C by using a Protean IEF Cell (Bio-Rad Laboratories, Hercules, CA). The IPG strips were equilibrated at room temperature for 15 min in equilibration buffers I and II (Bio-Rad Laboratories, Hercules, CA). The second dimension was performed on 8–18% gradient gels and run by using a Protean II xi system (Bio-Rad Laboratories, Hercules, CA) at 30 mA/gel. The 2DE analysis was performed in duplicate for each LTL muscle from both, C and H group, during storage time (0, 4, and 7 days). The gels were stained with Coomassie Blue G 250 and, after destaining, acquired by Chemi Doc EQ system (Bio-Rad Laboratories) and subsequently analyzed with PDQuest 7.4.0 software (Bio-Rad Laboratories) to obtain information on the number of spots per gel, the isoelectric point (pI), molecular weight (MW), volume, area and intensity of each spot. The protein spots detect to differ between the two experimental groups were automatically matched among the gels using the spots of a master gel (virtual gel comprehensive of all matched and unmatched spots of all 2DE images) used as a reference. Landmark spots were used to confirm spot matching across all gels and manual verification was used to screen out any dust artefacts or incorrectly identified spots. The relative volume of each spot in a gel was quantitatively determined after background subtraction and normalization as a percentage of the total volume of all spots detected on the gel.

2.3.3. Identification of protein spots of interest by LC-MS/MS

Spots displaying statistically significant differences among dietary treatments and storage time (in the H group at 7 days of storage) were carefully excised from the preparative gels and then washed for 30 min with 50 mM NH_4HCO_3. Samples were digested overnight at 37 °C with trypsin (12.5 ng/mL, Promega). Then, peptides were extracted, dried under vacuum, and suspended in 15 μL of 0.1% formic acid for LC-MS/MS analysis.

Separations were conducted using LTQ-Orbitrap XL mass spectrometer (Thermo Fisher Scientific) coupled with a nano-HPLC Ultimate 3000 (Dionex – Thermo Fisher Scientific) and equipped with a home-made pico-frit column (75 μm I.D., 15 μm Tip, 100 mm, New Objective) packed with C18 material (Aeris peptide 3.6 μm XB-C18, Phenomenex). Extracted peptides were concentrated in 15 μL of 0.1% formic acid and then eluted using a linear gradient of ACN/0.1% FA (from 3% to 40% in 19 min), at a flow rate of 250 nL/min.

The LC-MS/MS spectra were searched using Mascot Search Engine server (version 2.2.4, Matrix Science) and Proteome Discoverer 1.4 (Thermo Fisher Scientific) software package aligned against the *Ovis aries* database (version Nov 2021, 70994 entries). Carbamidomethylation of Cys residues was set as static modification, while Met oxidation was set as variable modification. Precursor and fragment tolerance were set at 10 ppm and 0.6 Da, respectively. Data were filtered to keep into account only proteins identified with at least 3 unique peptides with high confidence (False Discovery Rate (FDR) < 0.01) and a coverage of $\geq$20% to accurately validate the proteins in each spot.

2.4. Bioinformatics analyses

Protein-protein interaction analysis of the differentially abundant proteins (DAPs) was carried out using the open-source STRING database v11.0 (https://string-db.org). Considering the *Ovis Aries* Gene Ontology (GO) limitation, the ovine gene Uniprot IDs were converted into the human orthologues EntrezGene ID to obtain the most complete information on each gene name (protein) prior to analyses as suggested by Gagaoua et al. [35]. Confidence intervals were set to 0.400 (medium confidence) and false discovery rate (FDR) stringency was set to 1% in order to obtain as many significant features as possible while incurring a relatively low proportion of false positives. The default interaction sources criteria for linkage used were: text mining, co-occurrence, co-expression, experimental evidence, databases, neighborhood, and gene fusion.

Subsequently, the gene names of the DAPs were uploaded on Metascape® (https://metascape.org) and on Bionic visualizations Proteomaps (http://bionic-vis.biologie.uni-greifswald.de/) open-source tools. The Metascape® open-source tool was used to investigate the pathways and enrichment of the processes though the Gene Ontology (GO) terms. The proteomaps allowed an in-depth overview of the protein pathways and cellular processes with a focus on individual protein functions. The visualization of affected pathways (and responsible proteins) is built automatically from the computerized proteome data and based on the "KEGG Pathways" gene classification. Hereby, individual proteins are shown as polygons and to emphasize the fold of regulation, polygon sizes reflect the fold of changes in abundances. Functionally related proteins are arranged in proximity and with a similar color.

2.5. Statistical analysis

Instrumental color parameters, metmyoglobin percentages, densitometry data of 1D SDS-PAGE protein bands, and 2DE volume spots were analyzed using the GLM procedure of SAS 9.3. The model included the dietary treatment (C: control and H: hazelnut skin) and the days of storage (0, 4 and 7 days) and their interaction (diet x storage) as fixed effects, while the individual lamb was included in the model as random effect. All effects were tested for statistical significance set at $P < 0.05$, and when significant effects were found, Fisher's LSD test was used for

comparison.

Furthermore, a multivariate regression approach on the standardized data was conducted on the relative abundance of 1D protein bands proteins as previously conducted [36,37] to explain the variation for each meat color parameter following the parsimony rule described by Gagaoua et al. [38,39]. In the models, the 13 protein bands quantified by densitometry and qualitatively identified by MALDI-TOF have been used as explanatory variable. The regression models were built using the abundance of the protein bands to overcome inaccuracy produced by the large amounts of data obtained by the 2DE image analysis with less repeatability. For the explanatory models, the option "optimal model" was used to achieve regression equations with highest r-squares values. We set the maximum number of proteins to be retained in the regression equations of each color parameter to 3 to meet to the principle of parsimony.

3. Results

3.1. Color stability and metmyoglobin accumulation in lamb muscle

The effects of dietary treatment and storage time (0, 4 and 7 days) on color traits, stability and metmyoglobin accumulation in lamb meat are reported in Table 1. Refers to dietary treatment, significant differences were found for lightness (L^*; $P < 0.001$), redness (a^*; $P < 0.01$), yellowness (b^*; $P < 0.01$), and Chroma (C*; $P < 0.01$) parameters, with the highest values in meat from lambs fed with hazelnut skin. During storage time a significant increase ($P < 0.001$) of L^*, b^*, and h° parameters and a decrease of a^*-values ($P < 0.01$) were observed in both groups. For C*-values, a decrease after 4 days of storage was observed in the meat of both groups. Considering the reflectance indexes, an effect of storage time was found. Particularly, a significant decrease of R630/R580 and KS572/KS525 ratios ($P < 0.001$) was observed after 4 days in both groups, while, an increase was found for KS610/KS525 ($P < 0.001$) ratio. For metmyoglobin accumulation, no significant differences were found as a consequence of dietary treatment, whereas a significant and progressive increase of metmyoglobin (MMb%; $P < 0.001$) during storage time was found in lamb meat from both groups, showing the highest values in meat after 7 days of storage.

3.2. One-dimensional electrophoresis (1D SDS-PAGE) of the sarcoplasmic muscle proteome

The densitometry analysis on the 1D SDS-PAGE sarcoplasmic proteins as affected by dietary treatment and storage time (0, 4 and 7 days) are reported in Fig. 1. Data evidenced that the sarcoplasmic protein profile was significantly affected by dietary treatment and storage time. Particularly, although at 0 day of storage meat from both, C and H groups, was characterized by a similar profile in terms of number and intensity of bands (23 protein bands), after 7 days of storage, only meat from the hazelnut group displayed an increase of protein bands (23 *vs* 28 for C and H groups, respectively). Among these and based on an internal reference map on muscle combined to MALDI-TOF analysis 13 proteins, mostly from glycolysis, has been identified with protein coverage >45% and number of unique peptides >10: TPI1, PKM, LDHA, ENO3, PGM1, GPI, PYGM, PGAM1, MB, CKM, ALDOA, GAPDH and PGAM2. Only five proteins were affected by the treatments considered in this study. Meat from the hazelnut group showed higher intensity of pyruvate kinase (PKM; $P < 0.001$) and glycogen phosphorylase (PYGM; $P < 0.001$) during all storage times compared to control group. In addition, meat from hazelnut group showed greater abundance of triosephosphate isomerase (TPI1; $P < 0.01$) at 0 and 4 days and phosphoglycerate mutase 1 (PGAM1; $P < 0.001$) after 0 day of storage time. On the contrary, glyceraldehyde-3-phosphate dehydrogenase (GAPDH) was significantly more abundant at 0 ($P < 0.05$) and 4 days ($P < 0.001$) of storage in control meat to the hazelnut one (Fig. 1). However, referring to storage time, meat from the hazelnut group showed a significant decrease of GAPDH ($P < 0.01$) and PGAM1 ($P < 0.05$) during storage time, whereas meat from the same group, displayed an increase of PYGM ($P < 0.05$) after 7 days of storage.

3.3. Two-dimensional electrophoresis (2DE) and bioinformatics analysis of the differentially abundant protein spots

The representative 2DE gel maps of the sarcoplasmic proteome of LTL muscle from lambs as affected by the different dietary treatments and storage times (0, 4 and 7 days) are shown in Fig. 2. Image analysis showed that, at 0 day of storage, the meat of lambs fed with hazelnut skin diet was characterized by a similar protein profile, in terms of number and intensity of spots (196 ± 0.08 *vs* 180 ± 0.10 in H and C, respectively). However, after 7 days of storage meat from lambs fed with hazelnut skin showed a higher number of spots compared to the control group (252 ± 0.15 *vs* 164 ± 0.11 in H and C, respectively).

The protein spots that were found to change significantly in their abundance as a result of the hazelnut skin dietary treatment and storage time (7 days) were excised from preparative gels and identified by LC-MS/MS. A total of 10 protein spots, corresponding to 41 proteoforms (gene names), were found to be differentially abundant (Table 2 and annotation of Fig. 3). The proteins were identified to belong to three major biological pathways, these being.

i) *central carbon biosynthesis* ($n = 11$ proteins; 2-phospho-D-glycerate hydrolyase "ENO1", pyruvate kinase "PKM", triosephosphate isomerase "TPI1", glyceraldehyde-3-phosphate dehydrogenase "GAPDH", 3-hydroxyisobutyrate dehydrogenase, mitochondrial "HIBADH", creatine kinase "CKM", fructose-bisphosphate aldolase "ALDOA", phosphoglycerate mutase "PGAM2", adenylate kinase isoenzyme 1 "AK1",

Table 1
Effect of the dietary treatment (C = control; H = hazelnut) and storage time (0, 4, and 7 days) on instrumental color parameters (lightness: L^*, redness: a^*; yellowness: b^*; chroma: C*; hue angle: h°; reflectance: R630/R580; color stability: KS572/KS525; KS610/KS525) and metmyoglobin: MMb percentages (means ± SEM) of *Longissimus thoracis et lumborum* muscle of lambs.

	C			H			SEM	Effects, *P*	
	0d	4d	7d	0d	4d	7d		Diet	Storage
L^*	45.1 ^{ab}	44.0 ^{b}	46.4 ^{a}	46.3 ^{b}	45.8 ^{b}	48.5 ^{a}	0.51	***	***
a^*	14.4 ^{a}	11.3 ^{c}	12.3 ^{b}	14.9 ^{a}	11.8 ^{c}	13.3 ^{b}	0.30	**	***
b^*	11.3 ^{b}	10.6 ^{b}	12.5 ^{a}	11.8 ^{b}	11.2 ^{b}	13.6 ^{a}	0.33	**	***
C*	18.3 ^{a}	15.5 ^{b}	17.6 ^{a}	19.1 ^{a}	16.3 ^{b}	19.0 ^{a}	0.43	**	***
h°	37.9 ^{c}	43.1 ^{b}	45.5 ^{a}	38.3 ^{c}	43.4 ^{b}	45.5 ^{a}	0.40	NS	***
R630/R580	1.8 ^{a}	1.5 ^{b}	1.5 ^{b}	1.8 ^{a}	1.5 ^{b}	1.5 ^{b}	0.02	NS	***
KS572/KS525	0.98 ^{a}	0.92 ^{b}	0.89 ^{c}	0.97 ^{a}	0.92 ^{b}	0.88 ^{c}	0.01	NS	***
KS610/KS525	0.42 ^{c}	0.50 ^{a}	0.47 ^{b}	0.41 ^{c}	0.48 ^{a}	0.43 ^{b}	0.01	NS	***
MMb %	41.6 ^{c}	48.8 ^{b}	51.3 ^{a}	42.8 ^{c}	48.8 ^{b}	51.7 ^{a}	0.73	NS	***

NS = not significant; ** $P < 0.01$; *** $P < 0.001$. a, b, c = $P < 0.05$ in the row (storage effect) of the same group.

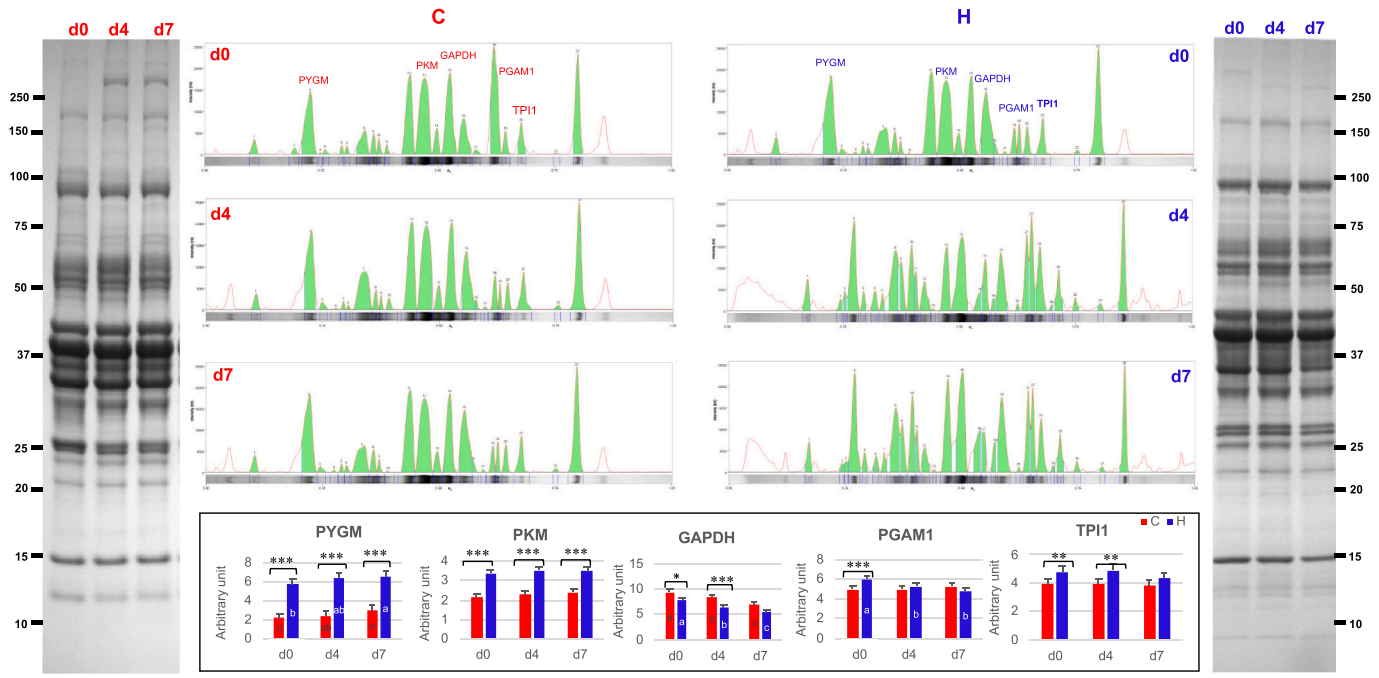

Fig. 1. Representative 1D SDS-PAGE gels and densitometry analyses of sarcoplasmic proteins from *Longissimus thoracis et lumborum* muscle of lambs as affected by dietary treatment (C: control; H: hazelnut) and storage time (0, 4 and 7 days). Abbreviations of the proteins found to be impacted by the treatments among 13 other proteins: PKM: Pyruvate kinase; PYGM: Glycogen phosphorylase; GAPDH: Glyceraldehyde-3-phosphate dehydrogenase; PGAM1: Phosphoglycerate mutase 1; TPI1: Triosephosphate isomerase. * $P < 0.05$; ** $P < 0.01$; *** $P < 0.001$.

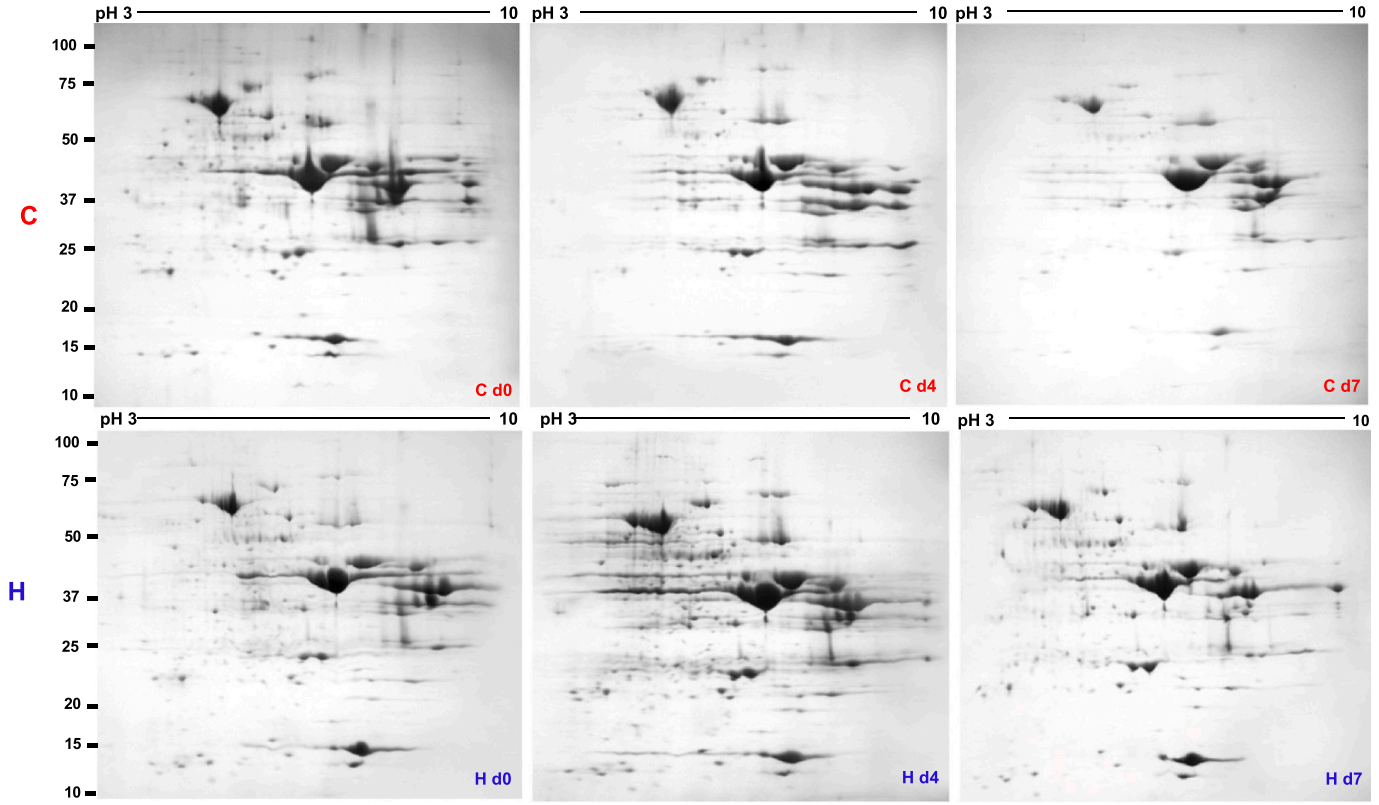

Fig. 2. Representative 2DE gels of the sarcoplasmic proteome from *Longissimus thoracis et lumborum* muscle of lambs as affected by dietary treatment (C: control; H: hazelnut) and storage time (0, 4 and 7 days).

phosphoglucomutase-1 isoform X2 "PGM1", phosphoglycerate kinase "PGK1");

ii) *biosynthesis* ($n = 7$ proteins; glutathione S-transferase "GSTM1", glutathione S-transferase "GSTM3", glutathione S-transferase "GSTM5", maillard deglycase "PARK7", peroxiredoxin-1

Table 2
Identified proteins by 2DE gels as different in the sarcoplasmic muscle proteome to be affected by dietary treatment.

Spot n.	Identified proteins	Gene name	Unipot ID	MW [kDa]	pI	Score	Coverage (%)	Matched peptides	Fold change [1]
1	14 kDa phosphohistidine phosphatase	PHPT1	A0A6P7DSX4	13.9	5.82	2573.06	52.00	7	+ 1.38
	Nuclear transport factor 2	NUTF2	A0A6P3E9M6	14.5	5.38	116.34	48.03	4	
	Apolipoprotein A-I	APOA1	A0A6P3TBJ5	30.3	5.97	259.99	46.42	12	
	2-iminobutanoate/2-iminopropanoate deaminase	RIDA	A0A6P3ESK7	14.3	8.12	122.06	42.34	5	
	Fatty acid-binding protein, heart isoform X1	FABP3	A0A6P3TBK2	14.8	6.57	153.40	33.83	5	
	Profilin	PFN1	A0A6P7EI30	15.0	8.28	78.43	22.14	3	
2	Nuclear transport factor 2	NUTF2	A0A6P3E9M6	14.5	5.38	625.07	79.53	7	+ 1.10
	Apolipoprotein A-I	APOA1	A0A6P3TBJ5	30.3	5.97	400.30	46.42	13	
	LIM domain-binding protein 3 isoform X13	LDB3	A0A6P7DGT7	31.0	9.19	92.38	22.97	5	
	Alpha-1-antitrypsin transcript variant 1	SERPINA1	I1WXR3	46.0	6.20	172.21	20.43	7	
803	60 kDa chaperonin	HSPD1	A0A6P7DQC9	60.9	5.87	8436.08	71.55	40	+ 1.08
	Fructose-bisphosphate aldolase	ALDOA	A0A6P7DGM3	39.4	8.19	618.84	34.89	13	
	Phosphoglucomutase-1 isoform X2	PGM1	A0A6P3DYV7	61.6	6.81	678.67	29.89	15	
	15-oxoprostaglandin 13-reductase	PTGR2	W5NRG0	38.4	5.39	196.22	23.93	7	
	Prohibitin	PHB	A0A6P3TWZ1	29.8	5.76	127.66	23.53	3	
	Pyruvate kinase	PKM	A0A6P3TIA1	58.0	7.53	715.76	23.16	13	
	Glyceraldehyde-3-phosphate dehydrogenase	GAPDH	A0A6P7DEU0	35.9	8.54	187.59	22.52	5	
	Creatine kinase	CKM	W5PJ69	43.0	7.15	196.33	22.05	7	
	2-phospho-D-glycerate hydrolyase	ENO1	A0A6P7EJI2	47.4	6.24	217.99	21.20	4	
2202	Maillard deglycase	PARK7	W5PK66	20.1	7.33	2596.94	61.38	15	+ 1.18
.	ATP synthase subunit d, mitochondrial	ATP5PD	B7P027	18.7	5.74	486.24	55.90	11	
	Peroxiredoxin-1	PRDX1	A0A6P3DYP3	22.2	8.40	364.36	52.26	9	
	Adenylate kinase isoenzyme 1	AK1	A0A6P9FQJ4	21.6	8.32	411.22	47.42	8	
	RAS oncogene family-like 7A	RAB7A	B2LYK6	23.5	6.70	314.54	46.86	9	
	Apolipoprotein A1	APOA1	W5NX51	29.5	6.20	167.37	27.41	6	
	Triosephosphate isomerase	TPI1	W5P5W9	22.8	5.63	184.22	23.36	4	
	Peroxiredoxin 2	PRDX2	C8BKC5	21.8	5.43	174.55	23.23	6	
	Phosphatidylethanolamine-binding protein 1	PEBP1	A0A6P3EBI4	21.0	7.49	113.17	22.99	3	
	Heat shock 27 kDa protein	HSPB1	A0A6P7DEW2	22.3	6.70	100.53	21.89	3	
2301	Triosephosphate isomerase	TPI1	A0A6M6R7Y5	30.6	6.55	2126.90	58.04	13	+ 1.11
	Maillard deglycase	PARK7	W5PK66	20.1	7.33	210.60	47.62	8	
	3-hydroxyisobutyrate dehydrogenase, mitochondrial	HIBADH	W5PHR0	34.8	7.90	1737.15	46.67	10	
	Apolipoprotein A1	APOA1	W5NX51	29.5	6.20	153.30	31.66	7	
	ATP synthase subunit d, mitochondrial	ATP5PD	B7P027	18.7	5.74	79.37	30.43	5	
	Carbonic anhydrase	CA3	W5PUC1	29.4	7.84	177.35	25.77	6	
	Prohibitin	PHB	A0A6P3TWZ1	29.8	5.76	34.49	23.53	3	
2401	Peroxiredoxin-6	PRDX6	A0A6P3CY24	25.1	6.38	2363.59	69.20	15	+ 1.22
	Triosephosphate isomerase	TPI1	A0A6M6R7Y5	30.6	6.55	1092.14	49.30	11	
	Proteasome subunit alpha type	PSMA6	B6EBS6	27.4	6.76	252.05	35.77	8	
	Phosphoglycerate mutase	PGAM2	A0A6P3EN06	28.8	8.90	612.51	29.64	9	
	Adiponectin (Fragment)	ADIPOQ	A0A0M4KDI9	13.7	8.60	107.25	27.64	3	
	Maillard deglycase	PARK7	W5PK66	20.1	7.33	89.66	24.87	4	
	3-hydroxyisobutyrate dehydrogenase, mitochondrial	HIBADH	W5PHR0	34.8	7.90	423.20	24.85	6	
	Carbonic anhydrase	CA3	W5PUC1	29.4	7.84	216.17	22.31	5	
	Apolipoprotein A1	APOA1	W5NX51	29.5	6.20	90.98	21.62	4	
3203	Maillard deglycase	PARK7	W5PK66	20.1	7.33	1459.79	64.02	12	+ 1.13
	Apolipoprotein A1	APOA1	W5NX51	29.5	6.20	316.52	45.17	12	
	Adenylate kinase isoenzyme 1	AK1	A0A6P9FQJ4	21.6	8.32	121.23	30.93	6	
	14 kDa phosphohistidine phosphatase	PHPT1	A0A6P7DSX4	13.9	5.82	177.18	21.60	3	
	Prefoldin subunit 3	VBP1	W5P0G8	22.5	6.28	127.48	20.30	4	
3808	Peroxiredoxin-6	PRDX6	A0A6P3CY24	25.1	6.38	288.65	30.80	7	+ 1.11
	Triosephosphate isomerase	TPI1	W5P5W9	22.8	5.63	161.96	23.83	4	
	2-phospho-D-glycerate hydrolyase	ENO1	A0A6P3YP53	47.3	6.58	934.54	21.20	7	
4202	Maillard deglycase	PARK7	W5PK66	20.1	7.33	1027.06	80.42	13	+ 1.07
	Apolipoprotein A-I	APOA1	A0A6P3TBJ5	30.3	5.97	206.98	40.38	9	
	Adenylate kinase isoenzyme 1	AK1	A0A6P9FQJ4	21.6	8.32	110.86	21.13	4	
4306	Triosephosphate isomerase	TPI1	A0A6M6R7Y5	30.6	6.55	8219.47	74.48	15	+ 1.20
	Maillard deglycase	PARK7	W5PK66	20.1	7.33	557.64	58.73	10	
	Carboxymethylenebutenolidase homolog	CMBL	A0A6P3EDS1	28.0	6.79	724.59	49.39	10	
	Uncharacterized protein	DHRS11	W5QAX4	28.3	7.40	415.38	34.62	8	
	ATP synthase subunit d, mitochondrial	ATP5PD	B7P027	18.7	5.74	213.52	31.06	8	
	High mobility group protein 1	HMGB1	A0A6P7EG22	24.9	5.74	132.47	30.23	6	
	Fructose-bisphosphate aldolase	ALDOA	A0A6P7DGM3	39.4	8.19	300.07	29.12	10	
	Apolipoprotein A1	APOA1	W5NX51	29.5	6.20	129.28	28.19	6	
	Glutathione transferase	GSTM5	A0A6P7EBK2	25.7	7.39	312.83	27.52	5	
	Peroxiredoxin-6	PRDX6	A0A6P3CY24	25.1	6.38	97.94	26.79	6	
	Glutathione S-transferase	GSTM1	A0A6P3TGT6	25.0	6.02	250.97	25.00	4	
	Persulfide dioxygenase ETHE1, mitochondrial isoform X1	ETHE1	A0A6P7ES27	27.8	7.25	341.86	24.41	6	
	Peroxiredoxin-1	PRDX1	A0A6P3DYP3	22.2	8.40	87.11	22.61	4	
	Proteasome subunit alpha type	PSMA6	B6EBS6	27.4	6.76	149.77	21.95	5	

(*continued on next page*)

Table 2 (*continued*)

Spot n.	Identified proteins	Gene name	Unipot ID	MW [kDa]	pI	Score	Coverage (%)	Matched peptides	Fold change [1]
	Phosphoglycerate kinase	PGK1	B7TJ13	44.5	8.27	435.58	20.62	8	
	Glutathione S-transferase	GSTM3	A0A6P3TM19	26.8	7.24	169.77	20.00	4	

[1] + is more abundant in the H group than C.

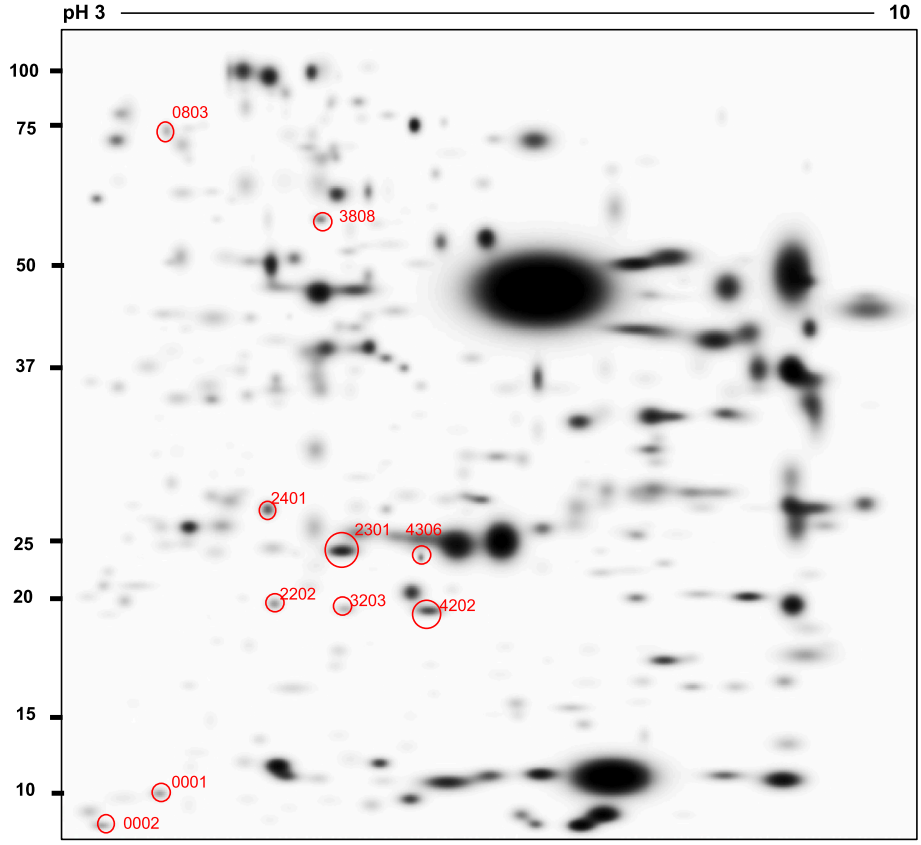

Fig. 3. Representative 2DE map of the sarcoplasmic proteome highlighting the differentially abundant proteins (see Table 2 for the identity of the proteins in each spot).

"PRDX1", peroxiredoxin 2 "PRDX2", Peroxiredoxin-6 "PRDX6"); and.

iii) *immune and endocrine system* ($n = 4$ proteins; fatty acid-binding protein, heart isoform X1 "FABP3", adiponectin (Fragment) "ADIPOQ", apolipoprotein A1 "APOA1", alpha-1-antitrypsin transcript variant 1 "SERPINA1").

It is worthy to note that the central carbon metabolism and biosynthesis pathways had close interactions with each other and with the heat shock family proteins (heat shock 27 kDa protein "HSPB1" and 60 kDa chaperonin "HSPD1"). In fact, the network of interacting proteins generated using the STRING database (Fig. 4A) identified 41 nodes (proteins) in biological interactions and 149 edges (interactions). Only the 14 kDa phosphohistidine phosphatase "PHPT1", carboxymethylenebutenolidase homolog "CMLB", 15-oxoprostaglandin 13-reductase "PTGR2" and nuclear transport factor 2 "NUTF2" proteins showed no significant interactions with other proteins, but the large majority of proteins displayed interactions.

Further pathways were identified in the proteomaps (Fig. 4B) likely energy metabolism (ATP synthase subunit d, mitochondrial "ATP5PB"); oxidative enzymes (peroxiredoxin 2 "PRDX2" and carboxymethylenebutenolidase homolog "CMBL"); folding, sorting and degradation (proteasome subunit alpha type "PSMA6" and 60 kDa chaperonin "HSPD1"); neurodegenerative disease (maillard deglycase "PARK7"); signal transduction (heat shock 27 kDa protein "HSPB1"); vesicular transport (RAS oncogene family-like 7A "RAB7A"); cell growth and death (profilin "PFN1"); DNA maintenance (high mobility group protein 1 "HMGB1").

From the Metascape analysis, 15 significantly enriched GO terms were allowed to construct process enrichment networks and pathways (Fig. 5). The top 4 enriched term clusters (Fig. 5A) were: "ATP metabolic process (GO:0046034)", "cellular detoxification (GO:1990748)", "protein stabilization (GO: 0050821)" and "glutathione metabolic process (GO:0006749). These were followed by "detection of oxidative stress (GO:0070994)", "positive regulation of cytokine production (GO:0001819)", "small molecule catabolic process (GO:0044282), "negative regulation of catalytic activity (GO:0043086), "response to mercury ion (GO: 0046689)", "organophosphate biosynthetic process (GO:0090407), "negative regulation of intracellular signal transduction (GO:1902532), "anatomical structure homeostasis (GO:0060249), "regulation of translation (GO:0006417)", "lipid catabolic process (GO:0016042)". The network association between the representative enrichment terms and their functional enrichment is given in Fig. 5B, showing the extent of enrichment of the clusters contributing to each GO term.

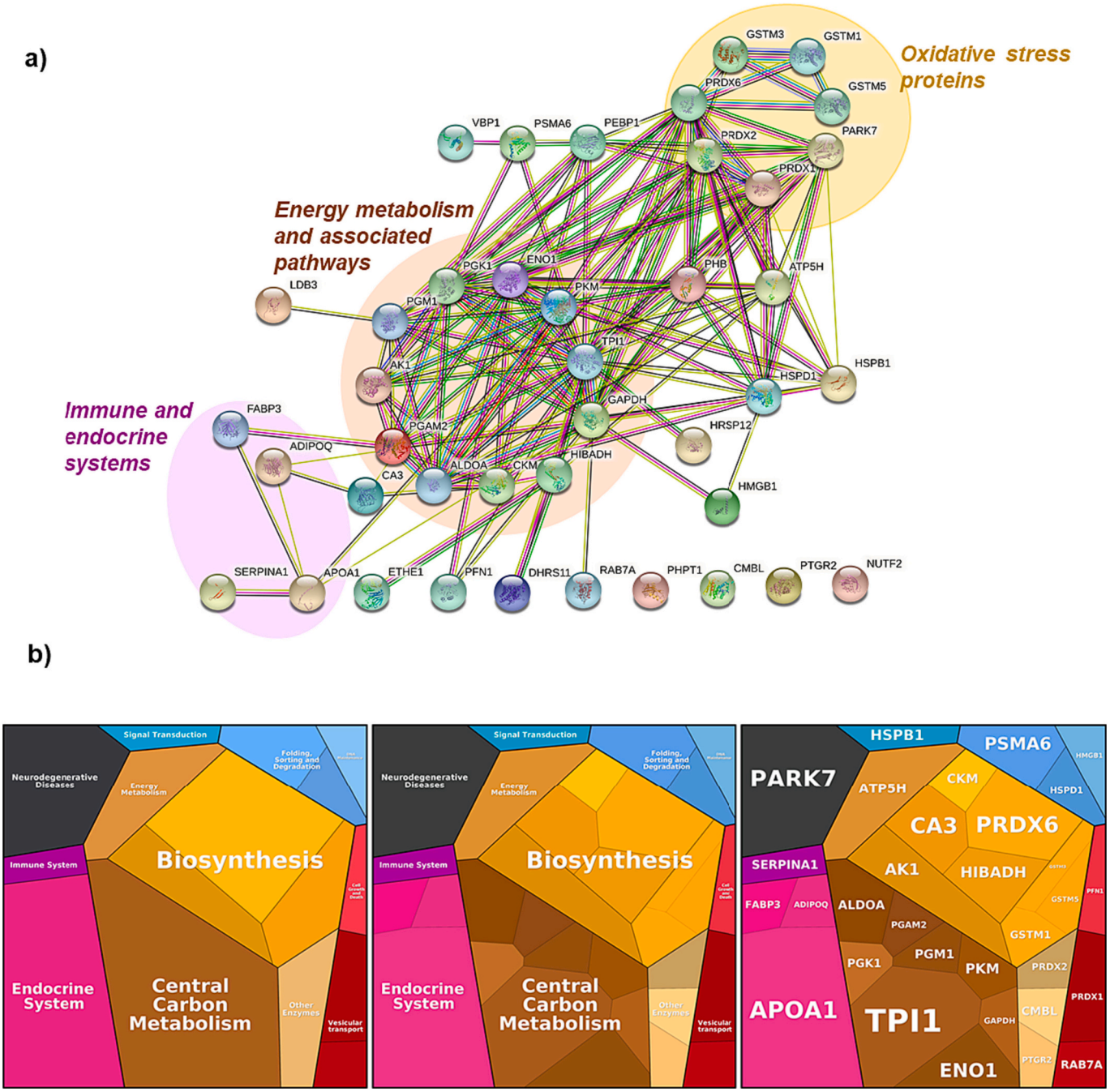

Fig. 4. Bioinformatics analyses of the differential proteins affected by the dietary treatment and storage time. A) Protein-protein interactions of the differentially abundant proteins using STRING database. The colored nodes represent query proteins and the first shell of interactors, whereas the connection lines indicate predicted functional annotations (light blue = evidence from curated databases; pink = experimentally determined evidence; green = gene neighborhood evidence; red = gene fusion; dark blue = gene co-occurrence evidence; light green = text mining evidence; black = co-expression evidence; purple = protein homology). B) Proteomaps pathways analysis of the differentially abundant proteins due to dietary treatment. Each polygon corresponds to a single KEGG pathway, and the size is proportional to its fraction in the total dataset. Tile colors represent different gene annotations. Genes/proteins that are closer on the maps and share the same color are closer in function. (For interpretation of the references to color in this figure legend, the reader is referred to the web version of this article.)

3.4. Explanatory models of color parameters with the sarcoplasmic protein abundances

The regression models of lamb meat using color parameters as dependent variables and the sarcoplasmic protein abundances, qualitatively identified by MALDI-TOF mass spectrometry as independent variables for each storage time are given in Table 3 and summarized in Fig. 6A. Considering all models, the thirteen proteins were all significantly correlated with color parameters and they explained between 18% and 75% of the variability, but varied in the number of their entrances (13 times for TPI1 *versus* 1 time for PGAM2) (Fig. 6A).

For lightness, at 0 day of storage, the model explained 60% of the variability ($P < 0.001$) entering PGM1 (negative), CKM and PGAM1 (both positive). At 4 days 53% of the variability ($P < 0.01$) was explained by PYGM (positive), PGM1 and MB (both negative); and at 7 days 71% of variability was explained by MB (negative), PGM1 and GAPDH (both positive).

The model of a^*, at 0 day, explained 22% of the variability by LDHA

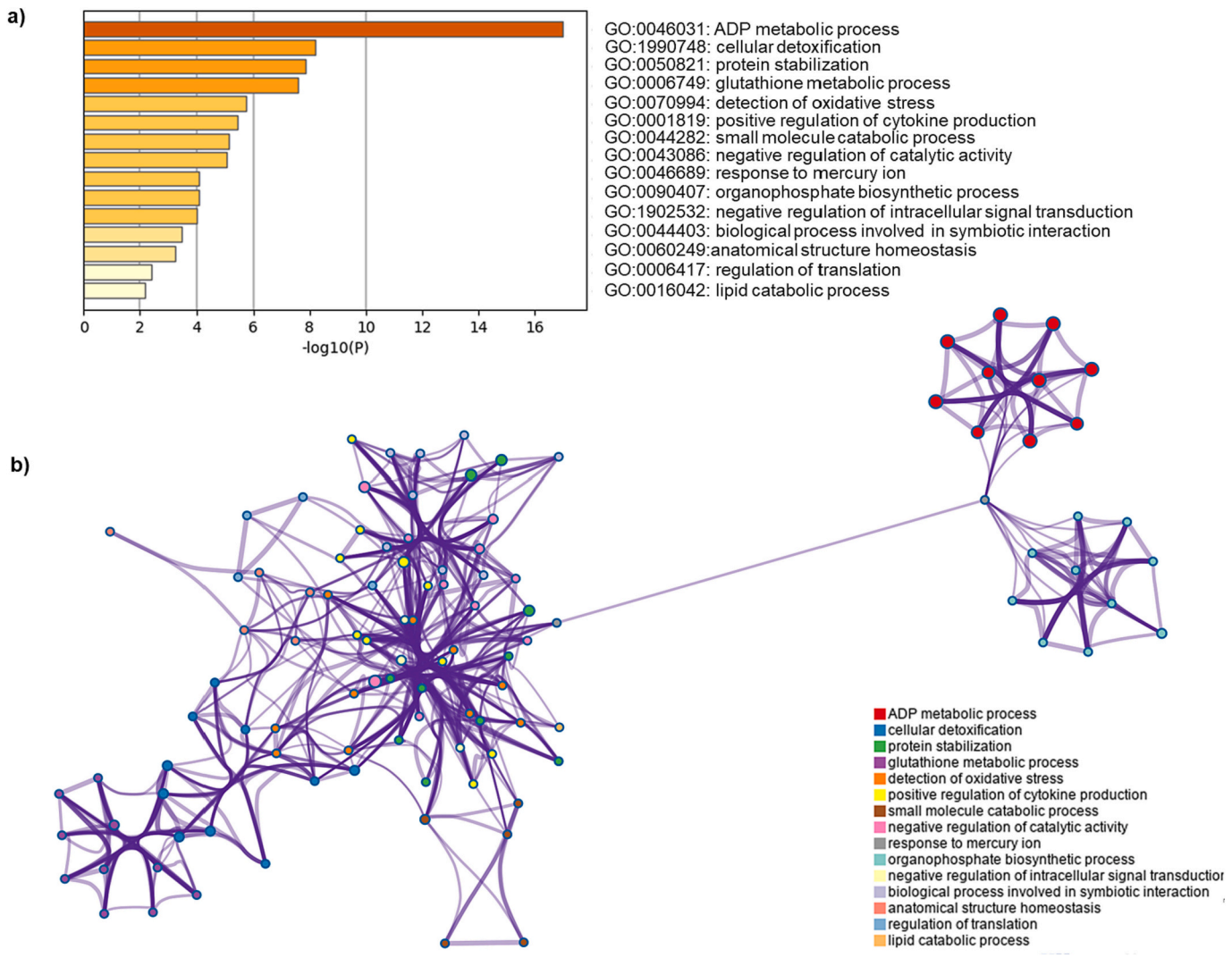

Fig. 5. Biological pathway and process enrichment analysis using Metascape® on the proteins identified in the sarcoplasmic proteome extract of lambs to be changing due to hazelnut dietary treatment. A) Functional enrichment analysis based on the list of 15 significant Gene Ontology (GO) terms. The bar graphs highlight the top enriched terms (functional clusters) across the protein lists colored according to *P* values: terms with a *P* value < 0.01, a minimum count of 3, and an enrichment factor > 1.5. B) Networks of pathways and process enrichment cluster analysis based on the identified differentially proteins.

(negative), ALDOA and TPI1 (both positive); at 4 days explained 60% of the variability ($P < 0.001$) by PKM, ENO3 and TPI1 (all negative); and after 7 days of storage, 74% of the variability ($P < 0.001$) was explained by GPI, ENO3 and TPI1 (all positive).

The *b** model explained 34% of the variability at 0 day of storage by PYGM, CKM and PGAM1 (all positive); at 4 days 42% of the variability ($P < 0.05$) by PKM, ENO3 and TPI1 (all negative) and after 7 days of storage 58% ($P < 0.01$) of the variability was explained by GPI, ENO3 and TPI1 (all positive).

Refers to C*, the model explained, that at 0 day, the 21% of the variability by PYGM (positive), LDHA (negative) and TPI1 (positive); after 4 days of storage the 45% ($P < 0.05$) by PKM, ENO3 and TPI1 (all negative) and the 61% of the variability ($P < 0.001$) by GPI, PGAM1 and TPI1 (all positive) at 7 days. The hue angle explained, at 0 day of storage, the 61% of the variability ($P < 0.001$) by PYGM, CKM and PGAM1 (all positive); at 4 days 26% of the variability was explained by PYGM (positive), PGM1 and MB (both negative); and at 7 days, 37% ($P < 0.05$) by PGM1 (positive), PKM and LDHA (both negative).

Considering the color stability parameters, the model of R630/R580 explained 21% and 28% of the variability at 0 and 4 days of storage, respectively. However, these models were weakly significant. After 7 days of storage, 65% of the variability ($P < 0.001$) was explained by GPI, PGAM1 and MB (all positive). The model of KS572/KS525 explained, that at 0 day of storage, 43% of the variability ($P < 0.05$) by PYGM, GPI (both negative) and LDHA (positive); 22% after 4 days of storage by LDHA, TPI1 (both positive) and PGAM1 (negative); and at 7 days 32% of the variability was explained by PGM1 (negative), PKM and LDHA (both positive).

The KS610/KS525 model explained, at 0 day, the 33% of the variability by PYGM, LDHA and TPI1; at 4 days the 64% ($P < 0.001$) by PKM, ENO3 and TPI1 (all positive); at 7 days the 75% ($P < 0.001$) by GPI, ENO3 and TPI1 (all negative). Finally, the model of metmyoglobin explained, that at 0 day of storage, the 54% of the variability ($P < 0.01$) by GPI, GAPDH and MB (all positive); at 4 days the 18% by PGAM2 (positive), ALDOA and TPI1 (both negative); while, at 7 days, 39% ($P < 0.05$) was explained by PGM1 (positive), PKM and LDHA (both negative). The frequency of the entrance of the proteins in the regression equations explaining the variability of the nine color traits at the three storage times is given in Fig. 6A. The proteomaps of the 13 sarcoplasmic proteins involved in the models are given in Fig. 6B. The results revealed that most of these are mostly, as expected involved in the post-mortem glycolysis (energy metabolism), and only two proteins were related to carbohydrate and amino acid metabolisms.

Table 3
Regression equations of meat color traits using the identified proteins (lightness: L^*, redness: a^*, yellowness: b^*, chroma: C*, hue angle: h°, reflectance: R630/R580, color stability (KS572/KS525, KS610/KS525, and metmyoglobin (MMb) percentages) of *Longissimus thoracis et lumborum* muscle of lambs as affected by dietary treatment and storage time (0 , 4 and 7 days).

Dependent variable	Days	R^2	Entered indipendent variable	Regression coefficient	SE
			PGM1	−0.60	0.16
	0	0.60***	CKM	+0.60	0.22
			PGAM1	+0.57	0.23
			PYGM	+0.35	0.21
L^*			PGM1	−0.42	0.20
	4	0.53**	MB	−1.00	0.24
			PGM1	+0.38	0.17
			GAPDH	+0.18	0.16
	7	0.71***	MB	−0.62	0.19
			ALDOA	+0.31	0.23
	0	0.22^t	LDHA	−0.40	0.23
			TPI1	+0.45	0.23
			PKM	−0.70	0.24
a^*			ENO3	−1.48	0.30
	4	0.60***	TPI1	−0.57	0.21
			GPI	+1.27	0.22
			ENO3	+0.99	0.22
	7	0.74***	TPI1	+0.45	0.13
			PYGM	+0.37	0.22
	0	0.34^t	CKM	+0.72	0.29
			PGAM1	+0.91	0.31
			PKM	−0.63	0.29
b^*			ENO3	−1.23	0.35
	4	0.42*	TPI1	−0.74	0.25
			GPI	+0.94	0.28
			ENO3	+0.66	0.28
	7	0.58**	TPI1	+0.48	0.16
			PYGM	+0.31	0.24
			LDHA	−0.39	0.22
	0	0.21^t	TPI1	+0.44	0.25
			PKM	−0.69	0.28
			ENO3	−1.30	0.35
	4	0.45*	TPI1	−0.71	0.25
			GPI	+0.81	0.18
			PGAM1	+0.43	0.17
C*	7	0.61***	TPI1	+0.22	0.15
			PYGM	+0.59	0.17
	0	0.61***	CKM	+0.87	0.22
			PGAM1	+1.19	0.24
			PYGM	+0.58	0.27
h°			PGM1	−0.42	0.25
	4	0.26^t	MB	−0.70	0.30
			PGM1	+0.51	0.24
			PKM	−1.38	0.53
	7	0.37*	LDHA	−1.30	0.49
			PKM	+0.75	0.40
			CKM	−0.28	0.24
	0	0.21^t	MB	+0.82	0.42
			PKM	−0.35	0.32
			ENO3	−0.59	0.32
	4	0.28^t	ALDOA	+0.36	0.20
			GPI	+1.76	0.31
			PGAM1	+0.52	0.16
R630/R580	7	0.65***	MB	+1.26	0.30
			PYGM	−0.43	0.19
			GPI	−0.64	0.19
	0	0.43*	LDHA	+0.25	0.18
			LDHA	+0.24	0.21
			PGAM1	−0.43	0.21
	4	0.22^t	TPI1	+0.24	0.22
			PGM1	−0.54	0.25
			PKM	+1.32	0.55
KS572/KS525	7	0.32^t	LDHA	+1.14	0.51
			PYGM	−0.42	0.22
			LDHA	+0.48	0.21
	0	0.33^t	TPI1	−0.54	0.23
			PKM	+0.83	0.23
KS610/KS525	4	0.64***	ENO3	+1.57	0.28
			TPI1	+0.62	0.20
			GPI	−1.15	0.22
			ENO3	−0.91	0.22
	7	0.75***	TPI1	−0.55	0.12
			GPI	+1.68	0.41
			GAPDH	+0.47	0.20
	0	0.54**	MB	+0.98	0.38
			ALDOA	−0.41	0.25
			PGAM2	+0.43	0.26
	4	0.18^t	TPI1	−0.40	0.26
			PGM1	+0.61	0.23
			PKM	−1.55	0.52
MMb %	7	0.39*	LDHA	−1.21	0.48

t = tendency ($P < 0.1$); * $P < 0.05$; ** $P < 0.01$; *** $P < 0.001$.
The full names of the proteins can be retrieved from Uniprot database (https://www.uniprot.org/).

4. Discussion

Meat color is a highly variable characteristic on which prediction and monitoring is a challenging task for the meat industry. For fresh meat, the post-mortem changes of skeletal muscle constitute a complex biochemical process influencing color stability. Recently, Soldado et al. [13] highlighted the ability of the condensed tannins-based diet to modulate animal antioxidant status, and consequently, prevent oxidative damage that can affect the meat color variation. In this study, we examined the changes in the sarcoplasmic proteome of meat from lambs of comparable age and rearing conditions supplemented with hazelnut skin by-product in the context of circularity of feeding resources for small ruminants. The stored meat samples were assessed by means of gel-based proteomics and bioinformatics approaches to better understand the potential role of feeding strategies in modulating mechanisms of meat discoloration and oxidation processes. We further aimed to reveal protein patterns related to dietary treatment and identify biomarkers of color stability in lamb meat.

4.1. Effect of dietary treatment and storage time on meat color stability

Results evidenced that the dietary treatment with hazelnut skin affected the lamb meat color parameters by increasing the lightness and yellowness. Similar results were observed previously in LTL muscle of lambs fed with different tanniferous diets such as carob pulp, acacia leaves or sulla fresh herbage [40,41]. This finding could be related to the role of tannins in delaying the synthesis of heme pigment *via* the modulation of the microbial biosynthesis of vitamin B12 as suggested in earlier studies [41,42].

It is well known that storage time can affect meat color parameters, development, stability and metmyoglobin formation [43]. It is also known that the monitoring of a^* and chroma (C^*) reflect the myoglobin concentration as well as its redox state in meat [3,44]. Refers to storage 7 days and to both a^* and C* values, our data evidenced substantial color development in meat from lamb fed with hazelnut by-product, highlighting an increase in the vividness of color and, consequently a delay of the discoloration. These findings are to some extent in line with the previous knowledge [43]. More specifically, the greater decrease in a^* and C* values after 7 days of storage in the control group (15% *vs* 11% for a^* in C and H group, respectively; and 4% *vs* 0.52% for C* in C and H group, respectively), highlight the important role of diet supplementation in monitoring the post-mortem processes of color variation. The decrease in the redness (a^*) values at day 4 of storage can be a consequence of pH variation. In fact, negative relations have been observed in several studies, for instance, referring to the models conducted by Calnan et al. [45] and to the accumulation of certain metabolites on the

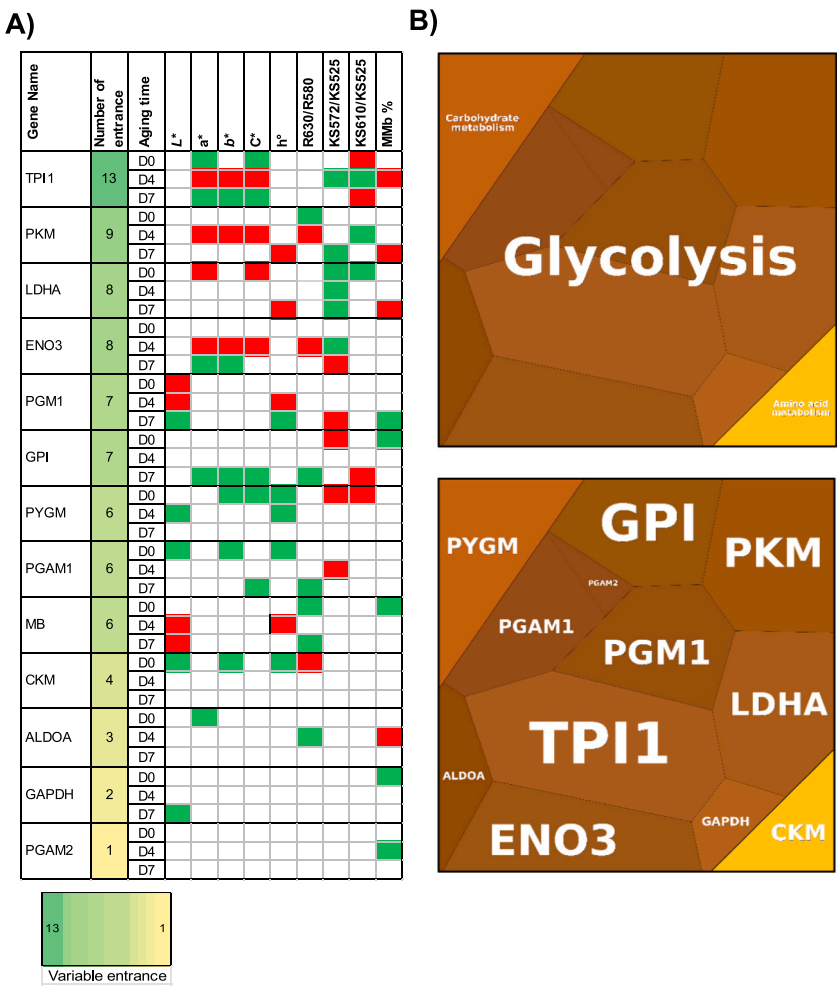

Fig. 6. Summary of the most important proteins retained in the explanation of color traits using multiple regression analysis. A) Regression models of meat color parameters and sarcoplasmic proteins abundances of *Longissimus thoracis et lumborum* muscle of lambs during storage (0, 4 and 7 days). The full names of the proteins can be retrieved from Uniprot database (https://www.uniprot.org/). The negative and positive correlations are in red and green, respectively. B) Proteomaps pathways analysis of the sarcoplasmic proteins involved in the models. (For interpretation of the references to color in this figure legend, the reader is referred to the web version of this article.)

surface of the meat as a response to water activity. Further studies are needed to go in-depth of this finding and understand the mechanisms.

The in-depth analysis of color stability using several descriptors mainly by evaluating the change in the predominant myoglobin forms over time, highlighted that storage time might impact redness and the accumulation of metmyoglobin content in the same manner in meat from both groups. This evidenced that the dietary treatment did not affect the trend of biochemical processes as further discussed below, for instance at the proteome level, the oxidation rates and the myoglobin chemistry over time.

4.2. Changes in the sarcoplasmic muscle proteome from hazelnut skin-based diet over storage time

Changes in the 1D SDS-PAGE protein bands intensities were observed in this study for proteins involved in the glycolysis and energy metabolism: PKM = Pyruvate kinase; PYGM = Glycogen phosphorylase; GAPDH = Glyceraldehyde-3-phosphate dehydrogenase; PGAM1 = Phosphoglycerate mutase 1; and TPI1 = Triosephosphate isomerase. These changes are in line with the current knowledge of the importance of glycolysis, energy metabolisms and associated pathways in the determination of meat color [1]. Indeed, proteins playing key roles in the post-mortem glycolysis in muscle are important cofactors in the reduction of enzymatic and non-enzymatic metmyoglobin formation [46]. Previous proteomics studies [22,23,28,29,31,47], including a recent integromics study in the context of beef [1], have linked the changes in glycolytic enzymes with myriad color parameters and several muscles differing in their color stability. These highlight the involvement of non-myoglobin proteins in the meat color determination and stability. For example, in the context of ovine meat, a recent study has linked the changes of PKM with color. The authors identified a positive correlation between redness and C* values and PKM intensity [28]. Thus, one can suggest PKM as a potential candidate for the monitoring of lamb meat color variation/discoloration. In the present study, the greater content of PKM protein together with the highest values of a^* and C* found in meat from lambs fed with hazelnut skin confirm the greater color stability. It confirms also the potential of using it as a candidate biomarker of lamb meat color as suggested for beef [1]. The importance of this enzyme could be explained by its role as a key rate-limiting enzyme in glycolysis [48] and in pH decline [49].

Among the other proteins from the glycolytic and associated pathways, GAPDH has been long recognized as a protein of interest due to its relationship with several meat quality traits (tenderness, WHC, pH and color) in beef [22,23,34,35], pork [50], horse [26] and lamb [51,52]. GAPDH is another key glycolytic enzyme, which catalyzes the production of NADH *via* glyceraldehyde 3-phosphate, also known as an important co-factor influencing the stability of meat color in post-mortem muscle thought the promotion of metmyoglobin reduction [5,44]. The association of GAPDH with meat color is muscle-dependent. Previous studies on different bovine and ovine muscles showed contrasting results depending on the contractile and metabolic properties of the muscles as well as of their color stability (labile *versus* stable). For example, Gao et al. [28] reported a positive correlation between GAPDH with a^* and C* values in color-stable LTL ovine muscle, while Wu et al. [23] found a negative correlation in the *Psoas major* muscle. In our study, meat from the hazelnut skin group displayed during storage a

decrease of GAPDH together with greater a^* values suggesting that a tannin-based diet, due to the content of antioxidant compounds, may act on post-mortem mechanisms by reducing the rate and extent of discoloration as well as the formation of metmyoglobin. On another hand and in line to an earlier study from our group on lambs fed with linseed and/or quinoa seed dietary supplementation [52], a significant role of diet in modulating meat tenderization rate supports the impact of pre-harvest feeding strategy on post-mortem biochemical processes and impact on the final outcomes.

However, the one-dimensional electrophoresis technique has some limitations, such as the coincidental co-migration of proteins with similar molecular weights in the same bands. For this reason, we further performed the 2DE combined with LC-MS/MS to address these shortcomings and to accurately identify the differentially abundant proteins between the two different dietary treatments. It is important to underline that different hydrophobic or extreme basic proteins could be under-represented and poorly resolved with 2DE techniques. Therefore, the combined approach applied in our study leads to overcoming these drawbacks and to provide a more comprehensive preliminary view of the changes in the sarcoplasmic proteome related to dietary treatment and revealing proteins of interest to better understand lamb meat color stability determination. However, for the regression models, we used the abundances of the protein bands to overcome the inaccuracy produced by the large amounts of data obtained by the 2DE image analysis (less repeatability). Indeed, the 2DE image analysis consists in detecting protein spots and match them among all the gels of the experiment, thus introducing considerable experiment variance due to the mismatching or missing spots. This is the major reason for which 1D gels were used to explore, in this preliminary study, before conducting a shotgun proteomics, the possibility of predicting multiple lamb meat color traits. To the best of our knowledge, densitometry data from 1D gels is what has been mostly admitted by the meat research community to explain quality traits [36,37] by means of regression models [38,39].

4.3. Functional roles of the changing proteins and their relevance to color determination

To further our understanding on the underlying mechanisms related to the impact of supplementation with hazelnut skin by-product on the color stability of lamb meat, we targeted the sarcoplasmic proteome changes using a classical 2DE proteomics approach. Meat from lambs fed hazelnut skins displayed a major increase of protein spots after 7 days of storage compared to the control, thus underlying the potential role of hazelnut antioxidant molecules in driving the biochemical processes determining meat quality variations during the post-mortem time, likely proteolysis. In fact, we could hypothesize an effect of the endogenous and reactive molecules of hazelnut skin by-product on the activity of endogenous muscle proteases known for their degradation activity, modification of protein expression and interactions during the muscle-to-meat conversion [49]. The appearance of high number of protein spots as a consequence of tenderization agrees with recent proteomics studies on beef [35].

In addition, the data evidenced, for the first time, the complexity of the mechanisms that are involved and their interconnectedness, mainly driven by energy metabolism and associated pathways followed by response to oxidative stress, and to lower extent immune and endocrine systems. More specifically, 41 proteoforms seemed in this study to contribute the biological mechanisms we identified to play role in the post-mortem metabolism related to color variation because of dietary treatment with hazelnut skin by-product. In addition to the above, putative protein biomarkers from glycolysis, energy metabolism and associated pathways were of pivotal role (ENO1, PKM, TPI1, GAPDH, HIBADH, CKM, ALDOA, PGAM2, AK1, PGM1 and PGK1), followed by response to oxidative stress and cell redox homeostasis (GSTM1, GSTM3, GSTM5, PARK7, PRDX1, PRDX2 and PRDX6), and to a lesser extent other with multifunctional roles but mainly involved in the immune and endocrine system (FABP3, ADIPOQ, APOA1 and SERPINA1). Interestingly, among these proteins, seven (ENO1, PKM, TPI1, GAPDH, CKM, ALDOA and AK1) were previously evidenced by proteomics to be related to lamb meat color parameters [27,28]. Whereas, when we compare our putative biomarkers with the recent beef integromics study of Gagaoua et al. [1], a total of 16 candidates (ENO1, PKM, TPI1, GAPDH, HIBADH, CKM, ALDOA, PGAM2, AK1, PGM1, PGK1, PARK7, PRDX1, PRDX2, PRDX6 and FABP3) can be validated. This study, allowed then to confirm previous knowledge and further proposed for the first time 6 new proteins belonging to oxidative stress and cell redox homeostasis (GSTM1, GSTM3, GSTM5) and immune and endocrine system pathways (ADIPOQ, APOA1 and SERPINA1) as candidate biomarkers of meat color in lamb.

4.4. Putative biomarkers of lamb meat color: glycolysis and energy metabolism pathway

Among the proteins identified involved in glycolytic processes, TPI1 was identified as the protein most influenced by dietary treatment due to the presence of 5 protein spots (proteoforms) in the sarcoplasmic proteome of meat from lambs fed hazelnut skin after 7 days of storage. This protein was further the top protein (13 times) retained in the regression equations built in this study to explain the measured color traits at different storage times. Triosephosphate isomerase is a key enzyme involved in energy generation for muscle cells that catalyze the conversion of dihydroxyacetone phosphate to glyceraldehyde 3-phosphate. This study is the first to validate the robustness of TPI1 in explaining lamb meat color variation. In other species, but mainly beef, TPI1 has been suggested as a biomarker of several quality traits including color [1,23,31,35,47,51]. In the current research, the greater abundance of TPI1 in the LTL muscle of the hazelnut group could be due to the greater capacity of this muscle to regenerate NADH for subsequent metmyoglobin reduction, hence allowing a better color stability [53]. The identification of several TPI1 protein spots in meat from the hazelnut group, together with the lowest decrease in a^* and C* values, highlight the important role of this protein in monitoring lamb meat discoloration and point out the reliability of TPI1 as a biomarker of lamb meat color variation or stability.

It was interesting to notice that the sarcoplasmic proteome of meat from the hazelnut skin group was also characterized by 3 proteoforms ascribed to AK1, a reversible enzyme, that plays an important role in the adenine synthesis and in maintaining muscle energy homeostasis [54]. Previous proteomics studies on lamb [28,29] and beef [22,23] identified this protein to be positively correlated with a^* and C*. Nair et al. [53] further reported a more abundance of this enzyme in bovine meat with a greater redness surface. In our study, the presence of these spots in meat from the H group confirms that monitoring its changes is a way to monitor muscle color variability, hence allowing us to suggest AK1 for further evaluation following the pipeline of biomarkers discovery [55].

ALDOA, ENO1 and HIBADH proteins (each identified in 2 spots) characterized also the meat of the H group. ALDOA and ENO1 have been very recently identified to be related to lamb meat color stability [28], while HIBADH is identified, for the first time in this study, as a candidate biomarker. However, it should be emphasized that only the proteomic study of Yang et al. [56] found a positive correlation between the 3-hydroxyisobutyrate dehydrogenase (HIBADH) and C* parameter in the bovine LL muscle packaged under a modified atmosphere. HIBADH is an important mitochondrial protein involved in the tricarboxylic acid cycle (TCA) related to post-mortem muscle metabolism, including valine degradation as reported in the biological mechanisms proposed by Gagaoua et al. [1]. The TCA cycle occurs within mitochondria and requires NAD and NADH (nicotinamide adenine dinucleotide reduced form) and the maintenance of the NAD/NADH ratio is necessary for efficient mitochondrial metabolism as well as for reducing metmyoglobin formation in meat [5,57,58]. The greater abundance of spots ascribed to HIBADH together with the highest values of a^* and C* found

in the lamb meat of the H group confirm the effectiveness of hazelnut skin dietary treatment in modulating the muscle biology and biochemical processes of color variation. However, further investigations are warranted on this protein to better understand the role of the TCA pathway in the mechanisms of lamb meat color and stability driven by animal feeding strategies.

4.5. Putative biomarkers of lamb meat color: oxidative stress and cell redox homeostasis pathways

The generation of reactive oxygen species (ROS) by mitochondria is known as one of the most deleterious causes of oxidative damage in muscle, involving different components of muscle cells [59,60]. PARK7, known also as DJ-1, is one of the chaperone proteins localized from the cytosol to mitochondria during oxidative stress [61] and plays an essential role in preventing the aggregation and denaturation of proteins. Refers to lamb meat proteome, Ma et al. [62] is the only study that reported an overabundance of PARK7 in muscles from callipyge mutation relating it to proteolysis and tenderness. Several earlier studies on bovine [39,47,53,56,58] and pork [7,63] evidenced major roles of PARK7 in color determination. Taken all together, the current knowledge of evidence highlight the important role of mitochondria in oxygen consumption and their reducing capacity, hence the final impact on meat color [64]. In this trial, the presence of six proteins (with a greater abundance) ascribed to PARK7 in the lamb meat from the H group after 7 days of storage support the role that hazelnut skin may play in the antioxidative properties of the meat during storage. In support of the above, the identification of peroxiredoxins (PRDX1, PRDX2 and PRDX6) in this trial is in agreement to the major roles ascribed to these proteins in meat color development [1]. These proteins are antioxidant enzymes able to reduce the oxides or superoxides produced by the metabolic pathways in the muscle, and consequently reduce the oxidative stress, hence protecting oxymyoglobin from the attack by peroxides [65,66]. Among peroxiredoxins, PRDX6 was identified in the integromics study of Gagaoua et al. [1] as the second top putative biomarker of beef color, while PRDX2 and PRDX1 were proposed as potential biomarkers of beef color stability. In our study, peroxiredoxins were more abundant in the reddest meat from lambs fed with hazelnut skin (3 spots for PRDX6; 2 spots for PRDX1 and 1 spot for PRDX2) thus confirming the antioxidant contribution to protect lamb meat against discoloration, hence leading to the better meat color stability. These findings also suggest that these proteins can be further consider for evaluation as candidate biomarkers for the explanation and/or the monitoring of lamb meat color.

4.6. Putative biomarkers of lamb meat color: immune and endocrine system pathway

Among the putative protein biomarkers belonging to the immune and endocrine system pathway, fatty acid-binding protein (FABP3) was the only previously identified as positively correlated to MRA in the LL muscle of Chinese Luxi yellow cattle [23]. ADIPOQ, SERPINA1 and APOA1 were for the first time evidenced in this trial, to drive lamb meat color variation. Particularly, among the putative biomarkers, the APOA1 was identified as the protein mostly influenced by dietary treatment due to the presence of 8 protein spots (proteoforms) in the sarcoplasmic proteome of meat from lambs fed hazelnut skin. Among apolipoproteins, at present only APOA5 and APOC3 genes were associated with pork meat quality [67]. Apolipoprotein A1 (APOA1) is the major protein component of high-density lipoprotein in the plasma membrane that displays anti-inflammatory properties [68]. It is known that as natural polyphenolic substances, tannins have been found to have antioxidants and anti-inflammation properties [69]. Therefore, it can be proposed that the presence of several spots ascribed to APOA1 in the sarcoplasmic proteome of H meat could be due to the role of tannins in the production of anti-inflammatory substances, therefore allowing an enhancement of the antioxidant properties of the muscle and consequently improving color stability. Thus, this can partly explain the greater a^* and C* values observed in the lamb meat from the animals fed with hazelnut skin by-product. APOA1 should be subjected to further evaluation using appropriate methods before its validation as a biomarker of lamb meat color stability.

Finally, in the sarcoplasmic proteome of lamb meat, further identified spots ascribed to SERPINA1 and ADIPOQ because of dietary treatment with hazelnut skin by-product. SERPINA1, also known as α1-antitrypsin, is a member of the serpins superfamily, the largest protease inhibitor family with multiple roles in intracellular and extracellular activities such as blood coagulation, fibrinolysis, apoptotic regulation and cell migration [38]. Although not yet extensively characterized in lamb meat [70] earlier studies discussed the important role of this superfamily of proteins in beef texture [71,72]. In pork, a positive correlation between serpins superfamily members and drip loss was reported [73]. Conversely, at present, no studies identified serpins, especially SERPINA1, as related to biochemical processes affecting meat color, thus further studies are needed to fully elucidate the role of the members of serpins in the determination of lamb meat color.

5. Conclusions

In-depth sarcoplasmic proteome study is useful for a better understanding of the role of feeding strategies on biochemical pathways and biological mechanisms of intrinsic meat qualities of lamb meat. Data from the current trial revealed the important role of tannin-diet supplementation in the improvement of meat oxidative stability by modulating the post-mortem processes linked with meat discoloration. Hazelnut skin dietary treatment led to better lamb meat color stability as evidenced by the increased redness and saturation index values. Proteomics and bioinformatics analysis on the sarcoplasmic proteome demonstrated that several pathways are involved in the post-mortem processes linked with color stability in lamb meat of the animals fed with hazelnut skin by-product in a context of circular economy. Glycolysis, followed by responses to oxidative stress, and other proteins involved in the immune and endocrine system were found as the major interconnected pathways that could act as potential predictors of lamb meat color stability. The identification of triosephosphate isomerase (TPI1) as one of the major predictors mostly retained in the regression equations, allow us to suggest it as a candidate biomarker of color stability in lamb meat in line with other meat species.

Funding

This research did not receive any specific grant from funding agencies in the public, commercial, or not-for-profit sector.

CRediT authorship contribution statement

Antonella della Malva: Conceptualization, Data curation, Formal analysis, Funding acquisition, Investigation, Methodology, Writing – original draft, Writing – review & editing. **Mohammed Gagaoua:** Data curation, Formal analysis, Investigation, Methodology, Writing – original draft, Writing – review & editing. **Antonella Santillo:** Conceptualization, Funding acquisition, Investigation, Writing – review & editing. **Martina di Corcia:** Formal analysis, Investigation, Methodology, Writing – review & editing. **Antonio Natalello:** Investigation, Writing – review & editing. **Agostino Sevi:** Conceptualization, Funding acquisition, Writing – review & editing. **Marzia Albenzio:** Conceptualization, Funding acquisition, Investigation, Writing – review & editing.

Declaration of Competing Interest

The authors declare no conflict of interest.

Data availability

Data will be made available on request.

Appendix A. Supplementary data

Supplementary data to this article can be found online at https://doi.org/10.1016/j.jprot.2023.104997.

References

[1] M. Gagaoua, J. Hughes, E.C. Terlouw, R.D. Warner, P.P. Purslow, J.M. Lorenzo, B. Picard, Proteomic biomarkers of beef colour, Trends Food Sci. Technol. 101 (2020) 234–252.

[2] R. Ramanathan, M.C. Hunt, R.A. Mancini, M.N. Nair, M.L. Denzer, S.P. Suman, G. G. Mafi, Recent updates in meat color research: integrating traditional and high-throughput approaches, Meat Muscle Biol. 4 (2) (2020).

[3] R. Mancini, M. Hunt, Current research in meat color, Meat Sci. 71 (1) (2005) 100–121.

[4] P.P. Purslow, R.D. Warner, F.M. Clarke, J.M. Hughes, Variations in meat colour due to factors other than myoglobin chemistry; a synthesis of recent findings (invited review), Meat Sci. 159 (2020), 107941.

[5] R. Ramanathan, S. Suman, C. Faustman, Biomolecular interactions in postmortem skeletal muscles governing fresh meat color: a review, J. Agric. Food Chem. 68 (46) (2020) 12779–12787.

[6] C. Faustman, Q. Sun, R. Mancini, S.P. Suman, Myoglobin and lipid oxidation interactions: mechanistic bases and control, Meat Sci. 86 (1) (2010) 86–94.

[7] T. Sayd, M. Morzel, C. Chambon, M. Franck, P. Figwer, C. Larzul, P. Le Roy, G. Monin, P. Chérel, E. Laville, Proteome analysis of the sarcoplasmic fraction of pig semimembranosus muscle: implications on meat color development, J. Agric. Food Chem. 54 (7) (2006) 2732–2737.

[8] P. Joseph, S.P. Suman, G. Rentfrow, S. Li, C.M. Beach, Proteomics of muscle-specific beef color stability, J. Agric. Food Chem. 60 (12) (2012) 3196–3203.

[9] R. Domínguez, M. Pateiro, P.E. Munekata, W. Zhang, P. Garcia-Oliveira, M. Carpena, M.A. Prieto, B. Bohrer, J.M. Lorenzo, Protein oxidation in muscle foods: a comprehensive review, Antioxidants 11 (1) (2021) 60.

[10] R. Ramanathan, L.H. Lambert, M.N. Nair, B. Morgan, R. Feuz, G. Mafi, M. Pfeiffer, Economic loss, amount of beef discarded, natural resources wastage, and environmental impact due to beef discoloration, Meat Muscle Biol. 6 (1) (2022).

[11] W. Zhu, M. Han, Y. Bu, X. Li, S. Yi, Y. Xu, J. Li, Plant polyphenols regulating myoglobin oxidation and color stability in red meat and certain fish: a review, Crit. Rev. Food Sci. Nutr. (2022) 1–13.

[12] S. Anusha Siddiqui, N.A. Bahmid, C.M. Mahmud, F. Boukid, M. Lamri, M. Gagaoua, Consumer acceptability of plant-, seaweed-, and insect-based foods as alternatives to meat: a critical compilation of a decade of research, Crit. Rev. Food Sci. Nutr. (2022) 1–22.

[13] D. Soldado, R.J. Bessa, E. Jerónimo, Condensed tannins as antioxidants in ruminants—effectiveness and action mechanisms to improve animal antioxidant status and oxidative stability of products, Animals 11 (11) (2021) 3243.

[14] G. Luciano, F.J. Monahan, V. Vasta, L. Biondi, M. Lanza, A. Priolo, Dietary tannins improve lamb meat colour stability, Meat Sci. 81 (1) (2009) 120–125.

[15] A. Priolo, G. Waghorn, M. Lanza, L. Biondi, P. Pennisi, Polyethylene glycol as a means for reducing the impact of condensed tannins in carob pulp: effects on lamb growth performance and meat quality, J. Anim. Sci. 78 (4) (2000) 810–816.

[16] J. Quijada, C. Drake, E. Gaudin, R. El-Korso, H. Hoste, I. Mueller-Harvey, Condensed tannin changes along the digestive tract in lambs fed with sainfoin pellets or hazelnut skins, J. Agric. Food Chem. 66 (9) (2018) 2136–2142.

[17] N.G. Taş, V. Gökmen, Bioactive compounds in different hazelnut varieties and their skins, J. Food Compos. Anal. 43 (2015) 203–208.

[18] A. Priolo, B. Valenti, A. Natalello, M. Bella, G. Luciano, M. Pauselli, Fatty acid metabolism in lambs fed hazelnut skin as a partial replacer of maize, Anim. Feed Sci. Technol. 272 (2021), 114794.

[19] M. Daghio, C. Viti, F. Mannelli, M. Pauselli, A. Natalello, G. Luciano, B. Valenti, A. Buccioni, A diet supplemented with hazelnut skin changes the microbial community composition and the biohydrogenation pattern of linoleic acid in the rumen of growing lambs, Ital. J. Anim. Sci. 20 (1) (2021) 1256–1263.

[20] R. Menci, L. Biondi, A. Natalello, M. Lanza, A. Priolo, B. Valenti, A. Bertino, M. Scerra, G. Luciano, Feeding hazelnut skin to lambs delays lipid oxidation in meat, Meat Sci. (2023) 109218.

[21] B. Picard, M. Gagaoua, Meta-proteomics for the discovery of protein biomarkers of beef tenderness: an overview of integrated studies, Food Res. Int. 127 (2020), 108739.

[22] A.C. Canto, S.P. Suman, M.N. Nair, S. Li, G. Rentfrow, C.M. Beach, T.J. Silva, T. L. Wheeler, S.D. Shackelford, A. Grayson, Differential abundance of sarcoplasmic proteome explains animal effect on beef longissimus lumborum color stability, Meat Sci. 102 (2015) 90–98.

[23] W. Wu, Q.-Q. Yu, Y. Fu, X.-J. Tian, F. Jia, X.-M. Li, R.-T. Dai, Towards muscle-specific meat color stability of Chinese Luxi yellow cattle: a proteomic insight into post-mortem storage, J. Proteome 147 (2016) 108–118.

[24] M. Gagaoua, E.C. Terlouw, B. Picard, The study of protein biomarkers to understand the biochemical processes underlying beef color development in young bulls, Meat Sci. 134 (2017) 18–27.

[25] M.D. Schulte, L.G. Johnson, E.A. Zuber, E.M. Steadham, D.A. King, E.J. Huff-Lonergan, S.M. Lonergan, L.G. Johnson, E.A. Zuber, E. Huff-Lonergan, Investigation of the sarcoplasmic proteome contribution to the development of pork loin tenderness, Meat Muscle Biol. 4 (1) (2020).

[26] A. Della Malva, A. Maggiolino, P. De Palo, M. Albenzio, J.M. Lorenzo, A. Sevi, R. Marino, Proteomic analysis to understand the relationship between the sarcoplasmic protein patterns and meat organoleptic characteristics in different horse muscles during aging, Meat Sci. 184 (2022), 108686.

[27] X. Gao, W. Wu, C. Ma, X. Li, R. Dai, Postmortem changes in sarcoplasmic proteins associated with color stability in lamb muscle analyzed by proteomics, Eur. Food Res. Technol. 242 (2016) 527–535.

[28] X. Gao, D. Zhao, L. Wang, Y. Cui, S. Wang, M. Lv, F. Zang, R. Dai, Proteomic changes in sarcoplasmic and myofibrillar proteins associated with color stability of ovine muscle during post-mortem storage, Foods 10 (12) (2021) 2989.

[29] Z. Li, M. Li, X. Li, J. Xin, Y. Wang, Q.W. Shen, D. Zhang, Quantitative phosphoproteomic analysis among muscles of different color stability using tandem mass tag labeling, Food Chem. 249 (2018) 8–15.

[30] B. Valenti, A. Natalello, V. Vasta, L. Campidonico, V. Roscini, S. Mattioli, M. Pauselli, A. Priolo, M. Lanza, G. Luciano, Effect of different dietary tannin extracts on lamb growth performances and meat oxidative stability: comparison between mimosa, chestnut and tara, Animal 13 (2) (2019) 435–443.

[31] M. Gagaoua, B. Picard, V. Monteils, Associations among animal, carcass, muscle characteristics, and fresh meat color traits in Charolais cattle, Meat Sci. 140 (2018) 145–156.

[32] K. Krzywicki, Assessment of relative content of myoglobin, oxymyoglobin and metmyoglobin at the surface of beef, Meat Sci. 3 (1) (1979) 1–10.

[33] D.A. King, M.C. Hunt, S. Barbut, J.R. Claus, D.P. Cornforth, P. Joseph, Y.H.B. Kim, G. Lindahl, R.A. Mancini, M.N. Nair, American meat science association guidelines for meat color measurement, Meat Muscle Biol. 6 (4) (2023).

[34] R. Marino, M. Albenzio, A. Della Malva, M. Caroprese, A. Santillo, A. Sevi, Changes in meat quality traits and sarcoplasmic proteins during aging in three different cattle breeds, Meat Sci. 98 (2) (2014) 178–186.

[35] M. Gagaoua, E.C. Terlouw, A.M. Mullen, D. Franco, R.D. Warner, J.M. Lorenzo, P. P. Purslow, D. Gerrard, D.L. Hopkins, D. Troy, Molecular signatures of beef tenderness: underlying mechanisms based on integromics of protein biomarkers from multi-platform proteomics studies, Meat Sci. 172 (2021), 108311.

[36] I. Zapata, H.N. Zerby, M. Wick, Functional proteomic analysis predicts beef tenderness and the tenderness differential, J. Agric. Food Chem. 57 (11) (2009) 4956–4963.

[37] C. Zhao, L. Zan, Y. Wang, M. Scott Updike, G. Liu, B.J. Bequette, R.L. Baldwin Vi, J. Song, Functional proteomic and interactome analysis of proteins associated with beef tenderness in Angus cattle, Livest. Sci. 161 (0) (2014) 201–209.

[38] M. Gagaoua, E.C. Terlouw, D. Micol, A. Boudjellal, J.-F.O. Hocquette, B. Picard, Understanding early post-mortem biochemical processes underlying meat color and pH decline in the longissimus thoracis muscle of young blond d'aquitaine bulls using protein biomarkers, J. Agric. Food Chem. 63 (30) (2015) 6799–6809.

[39] M. Gagaoua, V. Monteils, S. Couvreur, B. Picard, Identification of biomarkers associated with the rearing practices, carcass characteristics, and beef quality: an integrative approach, J. Agric. Food Chem. 65 (37) (2017) 8264–8278.

[40] A. Priolo, M. Lanza, L. Biondi, P. Pappalardo, O. Young, Effect of partially replacing dietary barley with 20% carob pulp on post-weaning growth, and carcass and meat characteristics of Comisana lambs, Meat Sci. 50 (3) (1998) 355–363.

[41] Q. Priolo, V. Vasta, Effects of tannin-containing diets on small ruminant meat quality, Ital. J. Anim. Sci. 6 (sup1) (2007) 527–530.

[42] H. Liu, K. Li, L. Mingbin, J. Zhao, B. Xiong, Effects of chestnut tannins on the meat quality, welfare, and antioxidant status of heat-stressed lambs, Meat Sci. 116 (2016) 236–242.

[43] L. Jeremiah, L. Gibson, The influence of storage temperature and storage time on color stability, retail properties and case-life of retail-ready beef, Food Res. Int. 34 (9) (2001) 815–826.

[44] P.P. Purslow, M. Gagaoua, R.D. Warner, Insights on meat quality from combining traditional studies and proteomics, Meat Sci. 174 (2021), 108423.

[45] H. Calnan, R.H. Jacob, D.W. Pethick, G.E. Gardner, Production factors influence fresh lamb longissimus colour more than muscle traits such as myoglobin concentration and pH, Meat Sci. 119 (Supplement C) (2016) 41–50.

[46] A. Bekhit, C. Faustman, Metmyoglobin reducing activity, Meat Sci. 71 (3) (2005) 407–439.

[47] W. Wu, X.-G. Gao, Y. Dai, Y. Fu, X.-M. Li, R.-T. Dai, Post-mortem changes in sarcoplasmic proteome and its relationship to meat color traits in M. semitendinosus of Chinese Luxi yellow cattle, Food Res. Int. 72 (2015) 98–105.

[48] R.J. Kraaijenhagen, M.C. van der Heijden, M. Streefkerk, G. Rijksen, G.C. de Gast, G.E. Staal, Hexokinase, phosphofructokinase and pyruvate kinase isozymes in lymphocyte subpopulations, Clin. Chim. Acta 140 (1) (1984) 65–76.

[49] E.M. England, S.K. Matarneh, T.L. Scheffler, C. Wachet, D.E. Gerrard, pH inactivation of phosphofructokinase arrests postmortem glycolysis, Meat Sci. 98 (4) (2014) 850–857.

[50] R. Lametsch, P. Roepstorff, E. Bendixen, Identification of protein degradation during post-mortem storage of pig meat, J. Agric. Food Chem. 50 (20) (2002) 5508–5512.

[51] M.N. Nair, S.P. Suman, M.K. Chatli, S. Li, P. Joseph, C.M. Beach, G. Rentfrow, Proteome basis for intramuscular variation in color stability of beef semimembranosus, Meat Sci. 113 (2016) 9–16.

[52] A. Della Malva, R. Marino, A. Santillo, G. Annicchiarico, M. Caroprese, A. Sevi, M. Albenzio, Proteomic approach to investigate the impact of different dietary supplementation on lamb meat tenderness, Meat Sci. 131 (2017) 74–81.

[53] M.N. Nair, S. Li, C.M. Beach, G. Rentfrow, S.P. Suman, Changes in the sarcoplasmic proteome of beef muscles with differential color stability during postmortem aging, Meat Muscle Biol. 2 (1) (2017).
[54] R. Zeleznikar, R. Heyman, R. Graeff, T. Walseth, S. Dawis, E. Butz, N. Goldberg, Evidence for compartmentalized adenylate kinase catalysis serving a high energy phosphoryl transfer function in rat skeletal muscle, J. Biol. Chem. 265 (1) (1990) 300–311.
[55] M. Gagaoua, The path from protein profiling to biomarkers: the potential of proteomics and data integration in beef quality research, in: IOP Conference Series: Earth and Environmental Science, IOP Publishing, 2021, p. 012029.
[56] X. Yang, S. Wu, D.L. Hopkins, R. Liang, L. Zhu, Y. Zhang, X. Luo, Proteomic analysis to investigate color changes of chilled beef longissimus steaks held under carbon monoxide and high oxygen packaging, Meat Sci. 142 (2018) 23–31.
[57] F. Kiyimba, S.D. Hartson, J. Rogers, D.L. VanOverbeke, G.G. Mafi, R. Ramanathan, Dark-cutting beef mitochondrial proteomic signatures reveal increased biogenesis proteins and bioenergetics capabilities, J. Proteome 265 (2022), 104637.
[58] M. Gagaoua, R.D. Warner, P. Purslow, R. Ramanathan, A.M. Mullen, M. López-Pedrouso, D. Franco, J.M. Lorenzo, I. Tomasevic, B. Picard, Dark-cutting beef: a brief review and an integromics meta-analysis at the proteome level to decipher the underlying pathways, Meat Sci. 181 (2021), 108611.
[59] A. Ouali, M. Gagaoua, Y. Boudida, S. Becila, A. Boudjellal, C.H. Herrera-Mendez, M.A. Sentandreu, Biomarkers of meat tenderness: present knowledge and perspectives in regards to our current understanding of the mechanisms involved, Meat Sci. 95 (4) (2013) 854–870.
[60] V. Sierra, M. Oliván, Role of mitochondria on muscle cell death and meat tenderization, Recent Pat. Endocr. Metab. Immune Drug Discov. 7 (2) (2013) 120–129.
[61] E. Junn, W.H. Jang, X. Zhao, B.S. Jeong, M.M. Mouradian, Mitochondrial localization of DJ-1 leads to enhanced neuroprotection, J. Neurosci. Res. 87 (1) (2009) 123–129.
[62] D. Ma, Q. Yu, V.E. Hedrick, B.R. Cooper, T.J.P. Sobreira, J.-H. Oh, H. Chun, Y.H. B. Kim, Proteomic and metabolomic profiling reveals the involvement of apoptosis in meat quality characteristics of ovine *M. longissimus* from different callipyge genotypes, Meat Sci. 166 (2020), 108140.
[63] A. Kwasiborski, T. Sayd, C. Chambon, V. Santé-Lhoutellier, D. Rocha, C. Terlouw, Pig longissimus lumborum proteome: part II: relationships between protein content and meat quality, Meat Sci. 80 (4) (2008) 982–996.
[64] R. Ramanathan, R.A. Mancini, Role of mitochondria in beef color: a review, Meat Muscle Biol. 2 (1) (2018).
[65] X. Jia, E. Veiseth-Kent, H. Grove, P. Kuziora, L. Aass, K. Hildrum, K. Hollung, Peroxiredoxin-6—a potential protein marker for meat tenderness in bovine longissimus thoracis muscle, J. Anim. Sci. 87 (7) (2009) 2391–2399.
[66] A.B. Fisher, Peroxiredoxin 6 in the repair of peroxidized cell membranes and cell signaling, Arch. Biochem. Biophys. 617 (2017) 68–83.
[67] Y. Hui, Y. Yang, R. Liu, Y. Zhang, C. Xiang, Z. Liu, Y. Ding, Y. Zhang, B. Wang, Significant association of APOA5 and APOC3 gene polymorphisms with meat quality traits in Kele pigs, Genet. Mol. Res. 12 (3) (2013) 3643–3650.
[68] M. Mangaraj, R. Nanda, S. Panda, Apolipoprotein AI: a molecule of diverse function, Indian J. Clin. Biochem. 31 (3) (2016) 253–259.
[69] Z. Tong, W. He, X. Fan, A. Guo, Biological function of plant tannin and its application in animal health, Front. Vet. Sci. 8 (2022) 1597.
[70] A. Della Malva, A. Santillo, A. Priolo, R. Marino, M.G. Ciliberti, A. Sevi, M. Albenzio, Effect of hazelnut skin by-product supplementation in lambs' diets: implications on plasma and muscle proteomes and first insights on the underlying mechanisms, J. Proteome 271 (2023), 104757.
[71] M. Gagaoua, K. Hafid, Y. Boudida, S. Becila, A. Ouali, B. Picard, A. Boudjellal, M. A. Sentandreu, Caspases and thrombin activity regulation by specific serpin inhibitors in bovine skeletal muscle, Appl. Biochem. Biotechnol. 177 (2015) 279–303.
[72] Y. Zhu, M. Gagaoua, A.M. Mullen, D. Viala, D.K. Rai, A.L. Kelly, D. Sheehan, R. M. Hamill, Shotgun proteomics for the preliminary identification of biomarkers of beef sensory tenderness, juiciness and chewiness from plasma and muscle of young Limousin-sired bulls, Meat Sci. 176 (2021), 108488.
[73] M.F. Te Pas, L. Kruijt, M. Pierzchala, R.E. Crump, S. Boeren, E. Keuning, R. Hoving-Bolink, M. Hortós, M. Gispert, J. Arnau, Identification of proteomic biomarkers in *M. longissimus* dorsi as potential predictors of pork quality, Meat Sci. 95 (3) (2013) 679–687.